Universidade do Minho
Escola de Ciências

Sara Emanuela Silva Nogueira

Development of new DODAX:MO:DC-Chol nanoparticles containing BRAF-siRNA for colorectal cancer therapy

Janeiro de 2015

Uminho | 2015 Sara Emanuela Silva Nogueira **Development of new DODAX:MO:DC-Chol nanoparticles containing BRAF-siRNA for colorectal cancer therapy**

Universidade do Minho
Escola de Ciências

Sara Emanuela Silva Nogueira

Development of new DODAX:MO:DC-Chol nanoparticles containing BRAF-siRNA for colorectal cancer therapy

Master thesis
Master in Biophysics and Bionanosystems

Supervisors:
Prof. Doutora Ana Arminda Lopes Preto de Almeida
Prof. Doutora Andreia Ferreira de Castro Gomes
Prof. Doutora Maria Elisabete Cunha Dias Real Oliveira

Janeiro 2015

Universidade do Minho, ___/___/_____

Assinatura: _____

Acknowledgments

In end of an important stage in my life, I would like to express my sincere appreciation for the support, availability and collaborations granted by several people who directly or indirectly contributed to this work.

Above all, I would like to thank Prof. Doutora Ana Preto, Prof. Doutora Elisabete Oliveira and Prof. Doutora Andreia Gomes for agreeing to be my advisors and the vote of confidence. Also, I want to thanks by all advices sent either professionally or personally, for the support, availability, attention, concern and especially for the tolerance and patience that had with me. It was an honor and a pleasure to work with you.

I want to express my gratitude to all my LBA and Photophysisc laboratory colleagues, especially to Ivo Lopes, Odete Gonçalves, Marta Casanova, Marisa Passos, Suellen, João, Rita, Patrícia, Fernando and so many others, for helping me in laboratory integration, for the joy, cheerfulness and companionship as all the teachings.

An especially grateful to Ana Oliveira that fleeing me the words to express all I much to thank. You'll be a great advisor.

I want to thank to my master colleagues, in especially to my dear Ana Hortelão whose always be there for me, no matter what.

I would also like to thanks my 'Pastelianos family', especially to Flávia Fernandes my best friend, who always be there for me and always heard my doubts and my frustrations supporting me even when they not perceived at all what I was talking about.

Finally, to my beloved family that always believed in me even when I didn't, always be there for me and never let me give up.

Abstract

Colorectal cancer (CRC) is a leading cause of cancer related mortality in the Western World. Preto A and collaborators demonstrated that BRAF is crucial for proliferation and survival of microsatellite instability (MSI) CRC with $BRAF^{V600E}$ but not of MSI CRC harboring KRAS mutations. This provides evidence supporting BRAF as a good target for therapeutic intervention in patients with sporadic MSI CRC harboring activating mutations in BRAF.

Gene therapy through siRNAs has been established as a new therapeutic alternative approach. Cationic liposomes have been extensively used among the nonviral methods used for gene delivery, being MO-based liposomes established as efficiently delivery systems for siRNAs. The aim of this thesis was to develop and characterize a novel DODAX:MO:DC-Chol based system for specific delivery of BRAF-siRNA in CRC cells for intravenous or local administration.

Our results demonstrated that all MO-based liposomal formulations were able to efficiently encapsulate siRNA. We could obtain stable lipoplexes of small size (100−160 nm) with a positive surface charge (>38 mV). We showed that DODAC-based liposomes exhibited higher fusogenic ability but more cytotoxicity in the CRC derived cell line RKO. Post-pegylation of the liposomes and lipoplexes decreased efficiently the surface charge of liposomes, and post-pegylated liposomes revealed a better internalization in RKO cells compared with non-pegylated ones. All MO-based liposomes showed low hemolysis, which is suitable for an intravenous injection. The analysis of the transfection efficiency and BRAF silencing of the lipoplexes DODAB:MO:DC-Chol containing BRAF-siRNA in RKO CRC cells, was not conclusive. Although further studies are needed, our preliminary results suggest that DODAB:MO:DC-Chol-BRAF-siRNA nanocarriers might be efficient in silencing BRAF expression in CRC cells.

In conclusion, the DODAB:MO:DC-Chol lipoplexes developed in this work might be promising nanovectors for siRNA delivery as a therapeutic approach for gene silencing in CRC.

Resumo

O cancro colo-retal (CCR) é a principal causa de morte, por cancro, no mundo ocidental. Preto A e colaboradores, demonstraram que o BRAF é crucial para a proliferação e sobrevivência dos CCRs com instabilidadade de microssatelites (MSI) com $BRAF^{V600E}$, mas não para os CCRs MSI com mutações do KRAS. Este facto fornece evidências que suportam o BRAF como um bom alvo para intervenção terapêutica em pacientes com CCR MSI esporádico com mutações do BRAF.

A terapia genética através de siRNAs tem sido estabelecida como uma nova abordagem terapêutica alternativa. Os lipossomas catiónicos têm sido extensivamente usados entre os métodos não virais para a entrega de genes, sendo os lipossomas baseados em MO estabelecidos como eficiêntes sistemas de entrega de siRNAs. O objetivo desta tese foi desenvolver e caracterizar sistemas DODAX:MO:DC-Chol para entrega específica de BRAF-siRNA em células de CRC para administração intravenosa ou local.

Os nossos resultados mostraram que todas as formulações de lipossomas baseadas em MO foram capazes de encapsular eficientemente siRNA. Obtivemos lipoplexos estáveis com pequenas dimensões (100-160 nm), com carga de superfície positiva (> 38 mV). Nós mostramos que os lipossomas baseados em DODAC exibiram maior capacidade fusogénica mas mais citotoxicidade na linha celular RKO derivada do CCR. A pós-pegilação dos lipossomas e lipoplexos diminuiu de forma eficiente a carga da superfície dos lipossomas, e os lipossomas pós-peguilados revelaram uma melhor internalização quando comparados com os não-peguilados, em células RKO. Todos os lipossomas contendo MO demonstraram uma baixa hemólise, o que é adequado para uma injecção intravenosa. A análise da eficiência de transfecção e do silenciamento do BRAF pelos lipoplexos DODAB:MO:DC-Chol contendo BRAF-siRNA nas células RKO de CCR, não foi conclusiva. Apesar de serem precisos outros testes, os nossos resultados preliminares, sugerem que os lipoplexos de DODAB:MO:DC-Chol-BRAF-siRNA poderão ser eficientes no silenciamento da expressão do BRAF em células de CCR. Em conclusão, os lipoplexos DODAB:MO:DC-Chol desenvolvidos neste trabalho poderão ser nanovectores promissores para entrega de siRNA, como uma abordagem terapêutica para o silenciamento de genes no CCR.

Table of contents

Table of equations

Table of Figures

Abbreviatons

CRC - Colorectal cancer

CIN - chromosomal instability

MSI - microsatellite instability pathway

DNA - Deoxyribonucleic acid

HNPCC - Hereditary nonpolyposis colorectal cancer

MSH2 - MutS homolog 2

hMLH1 - human mutL homolog 1

hPMS1 - human postmeiotic segregation 1

hPMS2 - human postmeiotic segregation 2

hMSH6 - human MutS homolog 2

TGF- β - Transforming growth factor β

MSI-H - Microsatellite instability- High

MSI-L - Microsatellite instability- Low

BRAF - V-RAF murine sarcoma viral oncogene homolog B

MSS - Microsatellite stable

KRAS - Kirsten rat sarcoma viral oncogene homolog

APC - Adenomatous polyposis coli

CG - Cytosine – Guanine

LOH - Loss of heterozygosity

CIMP - CpG Island Methylator Phenotype

5-FU - 5-fluorouracil

EGFR - Epidermal Growth Factor Receptor

MAPK - Mitogen-activated protein kinase

ERK - Extracellular-signal-regulated kinase

P3K - Phosphoinositide 3-kinase

Akt -Protein kinase B (PKB)

RAS - Rat sarcoma viral oncogene homolog

MEK - Mitogen-activated protein kinase kinase

Grb2 - Growth factor receptor-bound protein 2

GDP - Guanosine diphosphate

GTP - Guanosine triphosphate

VEGF-A - Vascular endothelial growth factor A

V - Valine

E - Glutamate

pDNA - DNA plasmid

ASO - Antisense oligonucleotide

RNAi - RNA interference

siRNA - small interfering RNA

shRNA - short hairpin RNA

miRNA - micro RNA

RISC - RNA-induced silencing complex

AVVs - Adeno-associated viruses

PEG - Poly(ethyleneglycol)

TE - Transfection efficiency

GI - Gastrointestinal

EPR - Enhanced permeability and retention

TaT - Trans-activating transcriptional activator

CL - Cationic lipid

SUV - Small unilamellar vesicles

LUV - Large unilamellar vesicles

GUV - Giant unilamellar vesicles

MLV - Multilamellar vesicles

CVC - Critical vesicular concentration

SNALPs - Stable nucleic acid lipid particle

LNP - Lipid Nanoparticles

HBV - Hepatite B vírus

PCL - Poly(epsilon-caprolactone)

MO - Monoolein

DODAB - Dioctadecyldimethylammonium bromide

T_m - Melting temperature

DOPE - Dioleoylphosphatidylethanolamine

DODAC - Dioctadecyldimethylammonium chloride

DC-Chol - DC-Cholesterol

I. Introduction

1. Nanomedicine: focus on cancer

Nanotechnology has been revolutionizing the development of different branches of science since Feynman developed the vision of manipulating and controlling things on a small scale creating the fields of nanoscience and nanotechnology. The application of nanotechnology in medicine is termed as Nanomedicine. Nanomedicine provides significant opportunities and new perspectives for novel and effective treatments in many disorders. Nanomedicine can be defined as the design and development of nanotherapeutics and/or diagnostic agents at the nanoscale range (with diameters ranging from 1 nm to 1000 nm), that can be encapsulated within biological systems, to targeted delivery of biomedical entities for the prevention, diagnosis and treatment of many diseases[1].

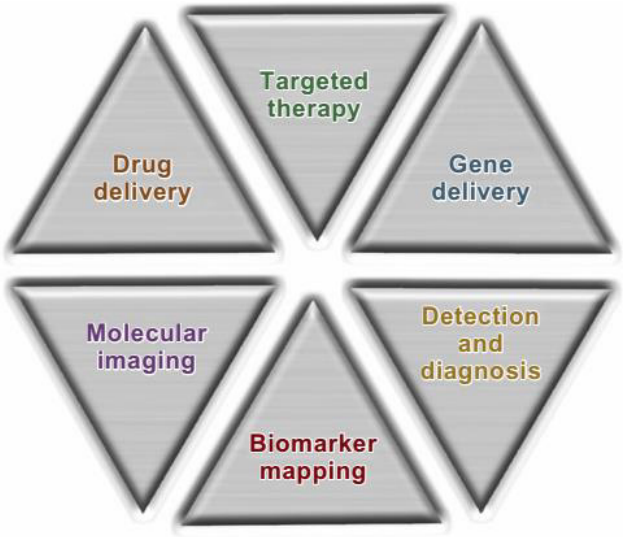

Figure 1 Biomedical applications of nanotherapeutics [2].

Cancer is a major public health problem all over the world. The incidence of cancer has been increasing in recent decades, and eradication of the major types of the disease remains an elusive clinical goal, largely due to the heterogeneous and idiosyncratic nature of individual cancers, and the inability to target therapeutics to neoplastic areas without damaging normal tissues[3].

New perspectives for cancer treatment have been achieved using innovative nanomaterials for the development of new nanotherapeutics as drug delivery or gene therapy.

2. Colorectal cancer: an overview

Colorectal cancer (CRC) is a leading cause of cancer related mortality in the Western World being anticipated that 136,830 new cases in 2014 would be diagnosed and approximately 50,310 individuals will die of the disease (http://seer.cancer.gov/).

CRC is characterized by a complex combination of epigenetic and genetic events. The sequence of genetic alterations inducing initiation and progression of the most CRCs are probably the best documented in the field of oncology[4]. Multiple studies have shown two major pathways in colorectal carcinogenesis, chromosomal instability (CIN) pathway (adenoma–carcinoma sequence) characterized by loss of alleles and microsatellite instability pathway (MSI).

MSI involves alterations of tandem repeats of simple deoxyribonucleic acid (DNA) sequences (microsatellites). MSI has been associated with hereditary non polyposis colorectal cancer (HNPCC) syndrome and mutations in genes encoding DNA mismatch repair enzymes, such as MSH2, hMLH1, hPMS1, hPMS2 and hMSH6, which appear to be responsible for the development of MSI in CRC. Moreover, mutations in microsatellites of target genes such TGF-β were identified in MSI tumors, which in turn, are present in sporadic CRC. In sporadic CRC, MSI-High (MSI-H) is present in 10-20 % and MSI-Low in 5-50 % of the cases. In about 80 % of MSI sporadic CRC are observed hipermethylation of hMLH1 promoter and are characterized by BRAF mutations[5]. Sporadic cases with MSI-H phenotype show different clinicopathological features compared with both MSS (microsatellite stable) and MSI-L, occurring predominantly close to colon and more frequently in female individuals. Histopathological features such mucinous or signet-ring cell differentiation and excess lymphocyte infiltrations as medullary features characterize these cancers[6].

MSI-L e MSS tumors frequently hold KRAS and p53 mutations and loss of heterozygosity (LOH) at 5q, 19p and 18q. Nevertheless, literature is controversial about the real differences between MSI-L and MSS tumors. It has been described the possibility of MSI-l tumors development and progression associated with both MSI and

CIN pathways. Approximately 30-40 % MSI-H sporadic cancers have adenomatous polyposis coli (APC) mutations and 36 % MSI-H tumors have p53 mutations. Certain CRC develop associated with MSI and APC or with p53 mutations[6,7].

CRC can also be classified into epigenetic subgroups. DNA methylation of cytosine bases in CG rich sequences, also called CIMP (CpG Island Methylator Phenotype), is the most extensively studied deregulated epigenetic mechanism in colorectal cancer. CIMP have a certain overlap with MSI and CIN and their classification is based on a panel of methylation markers (CIMP high, intermediate and low). CIMP high appear to be associated with MSI and BRAF mutations and has a better prognosis while CIMP low appear to be associated only with KRAS mutations[8].

In general, several genetic alterations affect genes encoding signaling pathway proteins in cancer, including membrane receptors or cytoplasmic protein kinases and phosphatases. The discovery of a role for these pathways in the initiation and progression of CRC has progressively lead to the development of new therapies, aiming to target key effectors of these pathways in order to reduce tumor growth.

2.1 Current colorectal cancer therapeutic

Surgery and/or chemotherapy still represents the standard treatment regimen for CRC therapy. Chemotherapy is either used as adjuvant setting or in order to decrease the size of the metastases, providing an opportunity to perform surgery at a later stage[9]. Current therapeutic regimens rely primarily on the cytotoxic agents 5-fluorouracil (5-FU), oxaliplatin and irinotecan, as well as the biologic agents targeting angiogenesis and the epidermal growth factor receptor (EGFR).

3. Epidermal growth factor receptor as target therapy of colorectal cancer

The EGFR and its downstream signaling pathways are involved in the development and progression of CRC, so both EGFR and some downstream components are appointed as targets for anticancer therapy. Two major signaling pathways activated by EGFR are the RAS-MAPK and PI3K-AKT pathway (Figure 2).

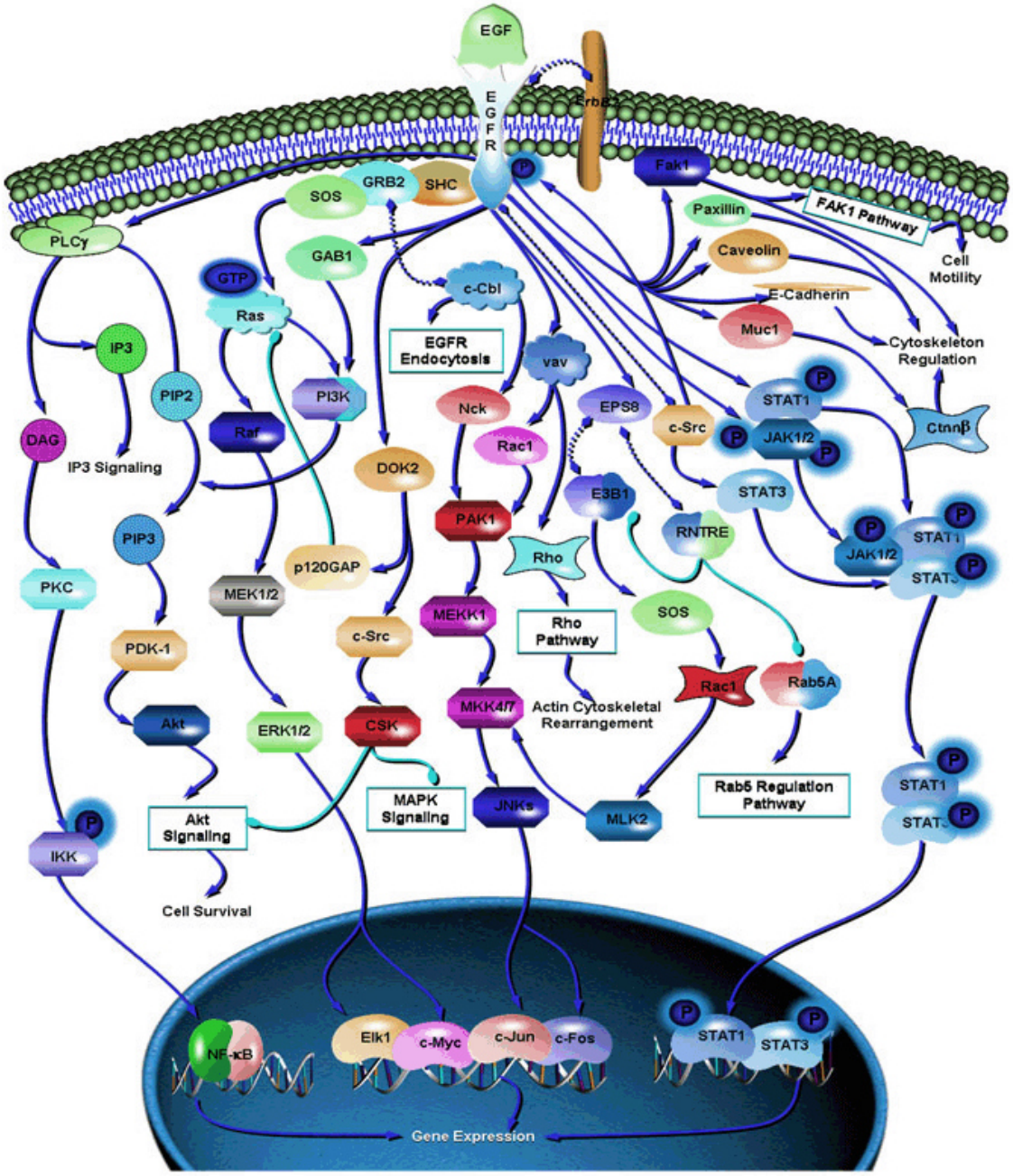

Figure 2. EGFR downstream signaling pathway. Adapted from SABiosciences.com.

In the RAS-RAF-MEK-MAPK, an adaptor protein complex composed by the growth factor receptor-bound protein 2 adapter protein (Grb2), which harbors a tyrosine phosphate-docking site, a RAS GDP/GTP exchange factor, then activates the RAS GTPase. Activated K-ras recruits and activates the serine protein B-raf, and subsequent phosphorylation and activation of MEK and then MAPK occurs, resulting in activation of transcription factors in the cell nucleus. The MAPK pathway regulates the expression of a large number of proteins involved in the control of cell proliferation, differentiation and apoptosis. The other axis of the EGFR signaling cascade is the PI3K-

AKT pathway, which results in cell growth, proliferation, and survival paralleling the RAS-RAF-MEK-MAPK signaling pathway, so both pathways are closely related and have some overlap[10].

The first generation of approved targeted compounds for the treatment of metastatic CRC were the anti-EGFR monoclonal antibodies Cetuximab and Panitumumab. Cetuximab is a chimeric IgG1 and Panitumumab is a human IgG2 monoclonal antibody that binds selectively to the EGFR binding site, thus blocking ligand–receptor interaction and inhibiting downstream signaling[11,12].

Another currently approach was Bevacizumab, an anti-angiogenic recombinant humanized monoclonal antibody that inhibits vascular endothelial growth factor A (VEGF-A). Anti-angiogenic treatment also has been associated to tumor invasion in melanoma[13], however, it remains unclear in case of colorectal cancer[14].

In the case of current EGFR-targeting antibodies, the lack of their efficiency is in part due to the fact that the tumor displays activating mutations of downstream oncogenes within the same pathway, namely the KRAS or BRAF genes.

3.1 BRAF as a target for sporadic colorectal cancer

BRAF is a key component of the RAS–RAF signaling pathway and a limiting step of several current therapies. BRAF mutation has been identified in a wide variety of human cancers, including sporadic CRC, melanomas and thyroid carcinomas[15]. Both BRAF and KRAS are prone to mutations in sporadic microsatellite unstable (MSI) CRC (31 – 45 and 18 % of cases, respectively)[16] and $BRAF^{V600E}$ mutation is inversely associated with oncogene KRAS[17]. $BRAF^{V600E}$ mutation promotes catalytic activity and is characterized by the substitution of thymidine by adenine at nucleotide 1799 leading to valine (V) substitution by glutamate (E) (referred to as V600E) at 600 codon in the activation segment[18]. $BRAF^{V600E}$ mutation is observed in 90 % of all BRAF mutations[16].

In sporadic CRC with a microsatellite instability (MSI) phenotype due to mismatch repair (MMR) deficiency, BRAF mutations were found in 31–45 % of the cases analyzed. In HNPCC tumors, BRAF mutations do not occur[17]. The association of BRAF with various cancers led to the investigation of BRAF pharmacological inhibitors and downstream proteins as therapies for individuals harboring BRAF-mutant tumors.

Sorafenib (Nexavar, or BAY 43-9006), was initially developed as a RAF inhibitor and tested for melanoma[19]. Recently, sorafenib was approved for the treatment of renal cell carcinoma and hepatocellular carcinoma, mainly because of its anti-angiogenesis effects rather than RAF inhibition[20,21]. Clinical responses to the highly selective small-molecule inhibitor of the BRAF (V600E) Vemurafenib and its analog PLX4720 differs widely, ranging from a response rate of approximately 80 % in melanoma to only 5 % in BRAF mutant CRC[22-25]. Other RAF inhibitors, such as LGX818, XL281, ARQ-736, RAF 265, Dabrafenib, RO5212054 and GSK-2118436, are being actively evaluated in preclinical models and early clinical trials including[26]. In phase III of clinical trial there are combinations between multiple inhibitors as Dabrafenib plus Trametinib, Vemurafenib plus Dacarbazine and/or GDC-0973, Sorafenib plus multiple combinations, which are reviewed in Huang *et al*, 2013[26].

Significant progress has been made in the development of RAF inhibitors, detection of common mutations, and understanding the role of these key signaling molecules in carcinogenesis. Multiple mechanisms have been suggested to support the clinical efficacy of BRAF. Interference on this pathway might achieve an anti-tumor effect, which is based in *in vitro* cell culture studies, xenograft tumor models, and clinical specimens[27,28]. Similarly to other cancer types, a survival plateau has been reached with combinations of cytotoxic drugs, increasing the demand for new approaches.

Preto *et al* demonstrated that BRAF inhibition by RNA interference in colorectal cancer cell lines induces apoptosis selectively in cells harboring the $BRAF^{V600E}$ mutation (CO115 and RKO), not having any effect in cells with $KRAS^{G13D}$. BRAF down-regulation promoted a decrease in ERK1/2 phosphorylation and cyclin D1 expression levels in BRAF-mutated cell lines in comparison to $KRAS^{G13D}$ mutated cells. Upon BRAF inhibition, they also found an increase in $p27^{Kip1}$ levels and a more pronounced decrease in the levels of anti-apoptotic protein Bcl-2, specifically in cell lines with $BRAF^{V600E}$[17]. This report provides evidence supporting BRAF as a good target for therapeutic intervention in patients with sporadic MSI CRC harboring activating mutations in BRAF but not in KRAS[17].

4. Gene therapy

The prospect of somatic *in vivo* gene therapy as an alternative approach to conventional drugs has generated significant interest. There are approximately 50,000 to 100,000 genes in the human genome and at least 30 % of colon cancers have been associated with defective genes, such as BRAF and KRAS genes.

Gene therapy involves the delivery of genetic materials into cells. Gene therapy can be performed to replace or correct the malfunction of a gene, or to trigger an immune response or to produce a therapeutic substance. Gene therapy has come to encompass the delivery of several distinct nucleic acids, including plasmid DNA (pDNA), antisense oligonucleotides (ASOs) and RNA interference (RNAi)-based systems [including small interfering RNAs (siRNAs), short hairpin RNAs (shRNAs) and microRNAs (miRNAs)] to target cells.

4.1 Gene therapy through RNA interference machinery

RNAi is a fundamental pathway in eukaryotic cells by which sequence-specific siRNA targets and induce the silencing of complementary mRNA[29,30]. RNAi is triggered by the presence of long pieces of double stranded RNA, that are cleaved in the cytoplasm of the cells by the Dicer enzyme into fragments of about 22 nucleotides long known as siRNA[31]. This shortcut reduces the potential for an innate immune interferon response and turn off the cellular protein expression through interaction of long pieces of double-stranded RNA with intracellular RNA receptor.

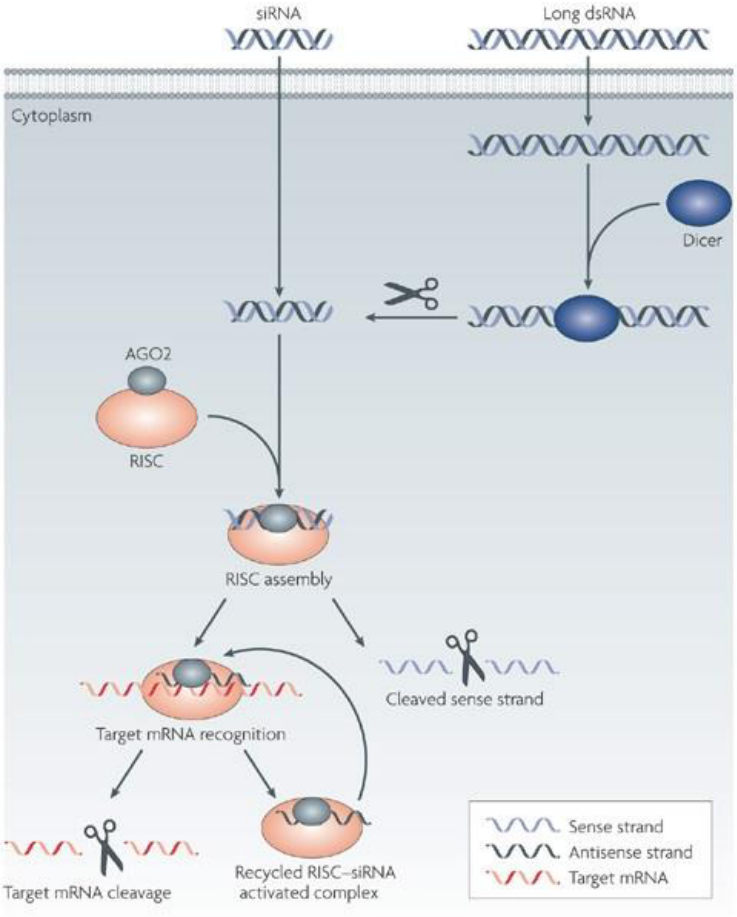

Figure 3. The mechanism of RNA interference (adapted from[32]). Long double-stranded RNA (dsRNA) is introduced into the cytoplasm, where it is cleaved into small interfering RNA (siRNA) by the enzyme Dicer. Also, siRNA can be introduced directly into the cell. The siRNA is then incorporated into the RNA-induced silencing complex (RISC), resulting in the cleavage of the sense strand of RNA by argonaute 2 (AGO2). The activated RISC–siRNA complex seeks out, binds to and degrades complementary mRNA leading to the target gene silence. The activated RISC–siRNA complex can then be recycled for the destruction of identical mRNA targets.

Chemically synthesized siRNA are double stranded RNAs (19-21 bp) with 2-nucleotide single-stranded overhangs at their 3' ends that mimic the cleavage products of the enzyme Dicer[33]. Upon introduction into the cell cytoplasm, siRNA is incorporated into a protein complex know as RNA-induced silencing complex (RISC) that integrates a multifunctional protein, Argonaut 2, unwinds the siRNA after siRNA sense strand cleavage[34]. The activated RISC complex containing the antisense strand of the siRNA, locates and cleaves mRNA at position between nucleotides 10 and 11 on the complementary antisense strand, relative to the 5'-end[35]. It then moves on to destroy additional mRNA targets preventing translation of the target mRNA into protein thus silencing the gene[36].

The RNAi machinery can be exploited to silence nearly any target gene or multiple genes, giving it a broader therapeutically potential than any small-molecule drug[32]. Indeed, therapeutic gene expression silencing, through naked synthetic siRNA, has already been under clinical trials in various diseases (Table 1)[33].

4.1 The challenges of *in vivo* small interference RNA delivery

As siRNA molecules are too large, hydrophilic and negatively charged to diffuse across the cell membranes and also require integration into the RNAi machinery, delivery material (vehicle) or chemical strategies are generally required to deliver therapeutic siRNA into the cell cytoplasm[32,37].

Common chemical modifications include replacement of the 2‘ OH group of ribose with -O-methyl or 2‘ fluorogroups, incorporation of locked or unlocked nucleic acids and substitution of phosphorothioate linkages in place of phosphodiester bonds[38]. Despite the effectiveness shown by the chemical modified siRNA, to achieve an effective delivery it is necessary to avoid siRNA degradation and immune recognition, thus the most common approach is the siRNA encapsulation into delivery vectors.

5. Properties of nanocarriers for delivery

After more than 10 years of RNAi technology discovery, the fundamental challenge of siRNA therapy remains the development of safe and effective delivery vectors. In general, an ideal siRNA delivery system must resist in the extracellular milieu preventing nonspecific interaction with proteins or non-target cells, avoiding recognition of immune system, allowing extravasation in order to reach target tissues and promote cell internalization.

5.1 Surface properties

The interaction between nanoparticles with the target cell and various serum components in the body depends significantly on the surface charge of the delivery systems. Firstly, positively charged nanoparticles promote the complex formation, called lipoplexes when cationic lipids are used, and compression of polyanionic nucleic acids of the siRNA through electrostatic interactions. Cationic systems can also promote internalization by adsorption to the negatively charged surface of the cells[32]. Several delivery systems rely on interactions with negatively charged serum proteins to allow

their uptake by target cells[39]. However, highly positive charged materials can induce nonspecific interactions and promote unfavorably aggregation[40]. Several approaches have been developed to increase nanovectors stability, including the incorporation of cholesterol and use of saturated lipids with higher transition temperatures[41]. Coating the delivery system with hydrophilic polymers (often polyethylene glycol (PEG)) avoids immune recognition[42,43]. PEG or other hydrophilic conjugates forms a barrier around nanoparticle controlling particle size, providing steric stabilization and protection from the physiological surroundings and allowing highest circulating half-lives, as well as reducing toxicity[44]. However, it has been reported that pegylation lowers the transfection efficiency (TE) of lipoplexes in different cell types[45,46], decreasing cellular association and entrapment in the endosomal compartments being appointed as the motive for the reduction of the transfection efficiency[47]. PEG-ceramides constitute a viable alternative approach to regular PEG-lipids. Besides the exchangeability of the PEG-ceramides, also the post-pegylation step is required to obtain pegylated lipoplexes with a high gene transfer capacity. In a post-pegylation with PEG-ceramides, a smaller amount of PEG-lipid was sufficient to avoid aggregation of the lipoplexes *in vitro*, compared to the pre-pegylated lipoplexes. The shorter the acyl chain of the PEG-lipid, the easier is the transfer of the PEG-ceramides from the lipoplexes to the cell membrane[48].

5.2 Toxicity

An effective and non-toxic siRNA delivery is the key challenge in delivery vehicles development. Both viral vectors and non-viral vectors are used for systemic delivery in clinical trials[49]. Particularly, 70% of gene therapy clinical trials carried out so far have used modified viruses such as retrovirus, lentiviruses, adenoviruses and adeno-associated viruses (AVVs)[33]. Despite of their high efficacy in gene therapy, viral vectors induce unacceptable levels of toxicity, such as carcinogenesis[50], immunogenicity[51], broad tropism[52]. In addition, difficulty in vector production and DNA packaging capacity are limitations associated with viral gene therapy[53]. Synthetic delivery vehicles, such as polymers and lipids, have been developed to offer alternatives to viral vectors for a non-toxic and effective gene therapy.

6. Barriers to small interference RNA delivery *in vivo*

6.1 Extracellular barriers

Local siRNA delivery to the intestine is an attractive strategy due to the relative ease of access by oral, rectal or endoscopic administration. Systemic administration can also be a reliable approach to intestinal siRNA delivery.

The successful of a local siRNA delivery is a significant challenge given the range of physiological and anatomical barriers associated with the gastrointestinal (GI) tract. Challenges to delivery of nucleic acids to the GI tract include the acidic environment of the stomach, components of intestinal fluids, intestinal and nuclease enzymes, presence of the mucus lining and the gut flora. In some conditions, the mucus layer can be reduced or missing in areas of acute inflammation, which can facilitate the access to the underlying epithelium. The inclusion of mucolytic agents prompted the delivery to target cells. Another barrier to intestinal delivery is the glycocalyx that is a size selective layer composed by glycoproteins and polysaccharides[41].

Systemic administration of synthetic delivery systems often results in accumulation in the organs of the reticuloendothelial system[54]. siRNA delivery particles larger than ~20 nm avoid glomerular filtration barrier through the kidneys[55]. Delivery systems that are not eliminated by degradation, phagocytosis, or glomerular filtration can leave the bloodstream by crossing endothelium to reach target tissues.

Some tumors present a combination of highly permeable endothelia and poor lymphatic drainage that can lead to increased accumulation of circulating nanoparticles in malignant tissue, a condition known as the enhanced permeation and retention effect (EPR)[56]. Moreover, it has been reported the success in targeting tumors through conjugation with ligands. The ligands used are known to bind to receptors that are overexpressed on the surface of the rapidly dividing cancer cells. For example, because of the high metabolic demands of rapid proliferation, many types of cancer cells overexpress transferrin and folate receptors, which makes conjugation with transferrin, folic acid or antibodies to these receptors, a successful targeting approach for engineered nanoparticles. Tumors targeting via folate-modified liposomes is an interesting, not so recent, approach since it is mediated by endocytosis which may contribute to bypass multidrug resistance. Daunorubicin and doxorubicin liposomes have been specifically delivered to tumor cells through folate receptor targeting

resulting in enhanced cytotoxicity[57,58]. Folate targeted vectors have been used for a specific delivery to tumors[59]. A recently international project, *Nanofol*, designed folate-based nanobiodevices for integrated diagnosis/therapy targeting chronic inflammatory diseases (http://www.nanofol.eu/). Nonetheless, as these receptors are expressed to some degree on many types of non-target cells, toxic off-target effects are not totally eliminated[60-62].

6.2 Cellular barriers to small interference RNA delivery

Cell membrane blocks diffusion of complexes larger than ~1 KDa. Several endocytic mechanisms can be engaged to facilitate the internalization of the delivery vehicles. The internalization mechanism determines intracellular trafficking of the nanoparticles. This is a dynamic process, through which siRNA nanocarriers are transported to different subcellular destinations that can be shuttled to lysosomes, recycled back to the plasma membrane or delivered into other subcellular compartments. In the majority of cases, material targeted to the lysosomes for degradation increases osmotic pressure inside of the endosome, resulting in its swelling and subsequent escape of siRNA from the endosome[63,64]. Ligands conjugated to the surface of engineered nanoparticles can influence the mode of cellular internalization. Ligands such as folic acid, albumin and cholesterol have been shown to be uptaked through caveolin-mediated endocytosis, whereas ligands for glycoreceptors promote clathrin-mediated endocytosis[63]. It has recently been suggested that lipoplexes internalization pathways are cholesterol-dependent and cholesterol affects their intracellular trafficking[65,66]. Engineered nanoparticles internalized through clathrin-mediated endocytosis are destined for the lysosomal compartment, whereas those internalized through a caveolin-mediated process are not. In clathrin-mediated endocytosis internalization, endosomal escape must occur before fusion with the lysosome to prevent degradation of the nanocarrier cargo under the harsh lysosomal conditions. Both caveolin and clathrin-mediated process requires endosomal escape to allow carrier access to the desired subcellular compartment, whether it is the cytosol, the mitochondria or the nucleus[67]. Alternatively, macropinocytosis can be engaged by incorporating cell-penetrating peptides, such as a trans-activating transcriptional activator (TaT) peptide into the design of engineered nanovectors[68]. The role(s) of particle size, shape and flexibility as well the ligand type,

density, multiplexing and region-specific labelling, in the internalization mechanism is yet to be better understood.

Endosomal escape is considered the major limitation step for efficient gene transfection. Cationic lipids (CL) in lipid based nanoparticles (LNPs) interact with anionic lipids and proteoglicans of the endosome, causing destabilization of the endosomal membrane[69]. It has been hypothesized that the buffering capacity of nanoparticles activates a proton influx that raises osmotic pressure inside the endosome, resulting in its swelling and subsequent release of the siRNA to the cytosol[64]. Regardless of the release mechanism, some reports have shown that nucleic acids remain largely trapped inside the endosomes and lysosomes with only a small fraction being released to the cytoplasm. Several approaches have been attempted to promote endosomal escape through the incorporation of non-bilayer forming-lipids, such as DOPE, cholesterol and/or lipids with pH sensitivity such as DODAP and CHEMS[70-72]. Other strategy is the Incorporation of molecules, such as the peptide mellitin with membrane lytic activity which disrupts the endosomal membrane and the amino acid histidine with pH-buffering capacity that bursts the membrane by increasing the endosomal osmotic pressure. The chemical drug chloroquine has also shown to promote nanocarrier endosomal escape through the phagolysosomal pH increase[73,74]. For many delivery systems, the precise mechanism of endosomal release is poorly understood as the exact intracellular trafficking pathways that affect delivery. Recently, Sahay and colleagues, reported that siRNA- based lipid delivery is substantially reduced as ~70% of the internalized siRNA undergoes endocytic recycling and exocytosis[75].

7. Non-viral lipid- based small interference RNA delivery

Many non-viral delivery systems have been developed for siRNA-based therapy. siRNA vector delivery research has been influenced by experiences on intracellular DNA delivery despite of the significant differences between siRNA and DNA, which include the lowest overall size and charge of siRNA, and the intracellular trafficking in cytoplasm, in the case of siRNA, and to nucleus, in the case of DNA. Therapeutic siRNA delivery clinical trials includes the injection of siRNA alone or in combination with a range of synthetic delivery vectors, including lipids and liposomes, polymers and conjugate delivery systems (Table 1).

Table 1. Non-viral siRNA vectors under clinical evaluation (Adapted[33]).

Delivery system	*Drug*	*Sponsor*	*Target Gene*	*Disease*	*Phase*	*Status*	*ClinicalTrials gov identifier*
Naked siRNA	ALN-RSV01	Alnylam Pharma	Nucleo-capsid gene of RCV	RSV infections	II	Completed	NCT00658086
	TD101	Pachyonychia Congenita Project	KRT6A(N171 Kmutation)	Pachyonychia congenita	I	Completed	NCT00716014
	AGN211745	Allergan	FLT1	Age-related macular degeneration and choroidal	II	Terminated	NCT00363714
	QPI-1007	Pharma Optic Quark	CASP2	Optic atrophy and non-arteric anterior ischemic optic neuropathy	I	Completed	NCT01064505
	I5NP	Quark Pharma	TP53	Kidney injury and acute renal failure	I	Completed	NCT00554359
				Delayed graft function and complications of kidney transplant	I/II	Active	NCT00802347
	PF-655 (PF-04523655)	Quark Pharma	DDIT4	Choroidal neovascularization, diabetic retinopathy and diabetic macular edema	II	Completed	NCT01445899
				Age-related macular degeneration	II	Completed	NCT00713518
	Bevasiranib	OPKO Health, Inc.	VEGFA	Diabetic macular edema	II	Completed	NCT00306904
				Macular degeneration	II	Completed	NCT00259753
	SYL1001	Sylentis S.A.	TRPV1	Ocular pain and dry eye syndrome	I/II	Recruiting	NCT01776658
	SYL040012	Sylentis S.A.	ASRB2	Ocular hypertension and open angle glaucoma	II	Completed	NCT01739244
	RXI-109	Rxi Pharma	CTGF	Cicatrix and scar prevention	I	Active	NCT01780077
				Hypertrophic scar	II	Recruiting	NCT02030275
				Keloid	II	Recruiting	NCT02079168
Lipid-based	ALN-VSP02	Alnylam Pharma	KIF11 and VEGF	Solid tumours	I	Completed	NCT01158079
	siRNA–EphA2–DOPC	MD Anderson Cancer Center	EPHA2	Advanced cancers	I	Active	NCT01591356
	Atu027	Silence Therapeutics	PKN3	Advanced solid cancers	I/II	Recruiting	NCT01808638
	TKM-080301	Tekmira Pharma Corporation	PLK1	Cancer	I/II	Recruiting	NCT01262235
	TKM-100201	Tekmira Pharma Corporation	VP24, VP35 and Zaire Ebola L-polymerase gene	Ebola virus infection	I	Terminated	NCT01518881
	PRO-040201	Tekmira Pharma Corporation	APOB	Hypercholesterolemia	I	Terminated	NCT00927459
	ALN-PCS02	Alnylam Pharma	PCSK9	Hypercholesterolemia	I	Completed	NCT01437059
	ALN-TTR02	Alnylam Pharma	TTR	TTR-mediated-amyloidosis	III	Recruiting	NCT01960348
	ND-L02-s0201	Nitto Denko Corporation	SERPINH1	Fibrosis	I	Completed	NCT01858935
CDP-based	CALAA-01	Calando Pharma	RRM2	Solid tumours	I	Terminated	NCT00689065

LOODER polymer siRNA-GalNAc conjugate	siG12D LODER	Silenseed Ltd.	KRAS	Pancreatic cancer	II	Active	NCT01676259
	ALN-TTRsc	Alnylam Pharma	TTR	TTR-mediated amyloidosis	I	Recruting	NTC01814839
					II	Recruting	NTC01981837
Dynamic-Poly-Conjugate	ARC-520	Arrowhead Research Corporation	Two conserved regions of Hbv transcrips	Hepatitis B	I	Recruting	NTC01872065
					II	Recruting	NTC02065336

ADRB2, adrenoceptor beta 2, surface; APOB, apolipoprotein B;CASP2, caspase 2, apoptosis-related cysteine peptidase; CDP, cyclodextrin polymer; CTGF, connective tissue growth factor; DDIT4, DNA-damage-inducible transcript 4 (also known as RTP801);EPHA2, EPH receptor A2;FLT1, fms-related tyrosine kinase 1 (also known as VEGFR1); GalNAc, N-acetylgalactosamine; HBV, hepatitis B virus;KIF11, kinesin family member 11; KRT6A, keratin 6A; PCSK9, proprotein convertase subtilisin/kexin type 9; PKN3, protein kinase N3; PLK1, polo-like kinase 1; RRM2, ribonucleotide reductase M2; RSV, respiratory syncytial virus; SERPINH1, serpin peptidase inhibitor, clade H, member 1 (also known as HSP47); siRNA, small interfering RNA, TP53encodes p53; TRPV1, transient receptor potential cation channel, subfamily V, member 1; TTR, transthyretin;

7.1 Lipid-based small interference RNA delivery

Unillamelar and multilamellar liposomes are widely used as pharmaceutical delivery systems. In aqueous environment, lipid amphiphiles, chemical compounds including a hydrophilic region, a polar headgroup, covalently linked to the hydrophobic region of one or more nonpolar hydrocarbon chains are capable of self-assembly forming uni-or multilamellar lipid bylayer enclosing an hydrophilic core, which can houses the nucleic acid cargo[76]. Liposomes are categorized in small unillamelar vesicles (SUV), large unilamellar vesicles (LUV), giant unilamellar vesicles (GUV) and multilamellar vesicles (MLV) (Figure 4).

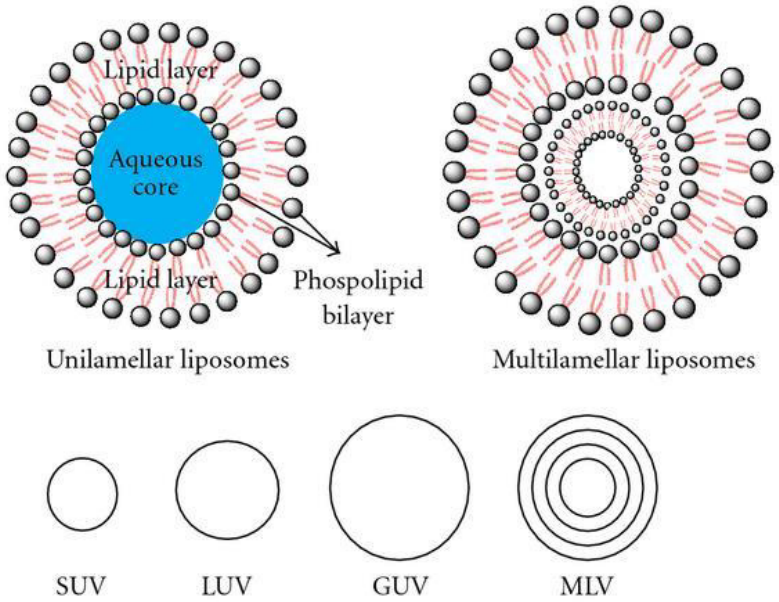

Figure 4. Schematic representation of basic structures and different types of liposomes. Small nillamelar vesicles (SUV), large unilamellar vesicles (LUV), giant unilamellar vesicles (GUV) and multilamellar vesicles (MLV).

This process of self-assembly occurs above the critical vesicle concentration (CVC) and is dependent on parameters such as pressure, temperature, phospholipid headgroup repulsion and phospholipid tail length[77]. Liposomes can be created using single or multiple types of lipids, which allows for additional flexibility when optimizing the physical and chemical properties of the nanoparticle[57].

Liposomes have been used for the delivery of nucleic acids for over 20 years, since the studies performed by Felgner and colleagues describing the ability of the cationic lipid DOTMA (N-[1-(2,3-dioleyloxy)propyl]-N,N,Ntrimethlyl ammonium chloride) to deliver both DNA and RNA into mouse, rat and human cell lines[78,79]. Several lipid-based vectors have been used to deliver therapeutic nucleic acids to and /or via intestine in animal models. The majority of *in vivo* studies have used commercially available cationic lipids, such as Lipofectin®, Lipofectamine® 2000 and DOTAP. However, liposomes have poor stability in the intestine and this could explain why the cationic polymers of the polysaccharide chitosan are among the most widely used delivery vectors for intestinal gene therapy research[41].

Lipid based-siRNA delivery is the most widely used strategy in clinical trials among polymers or conjugates (Table 1)[33]. One class of lipid-based siRNA delivery systems under clinical evaluation is AtuPLEX, which consists of a cationic lipid (AtuFECT01), a

helper lipid (DPhyPE) and a PEG–lipid (PEG–DSPE) in a 50:49:1 ratio with siRNAs. This formulation was shown to internalize into mouse vascular endothelium after intravenous injection[80]. The AtuPLEX-based formulation Atu027 features a siRNA that targets the protein kinase N3 (PKN3) transcript and is under evaluation for the treatment of patients with advanced solid cancer (NCT01808638)[81]. Another approach, consisting in siRNA encapsulation into neutral liposomes composed of DOPC, was attempted with siRNA–EphA2–DOPC formulation (NCT01591356)[82]. This siRNA delivery system targets EPHA2 (which encodes a tyrosine kinase) and is being evaluated in patients with advanced cancers.

Another class of lipid-based siRNA delivery systems under clinical evaluation are stable nucleic acid-lipid particles (SNALPs). SNALPs involve the encapsulation of nucleic acids into lipid-based nanoparticles (LNPs). The first SNALP formulation for siRNA delivery was reported in 2005 and targets the hepatitis B virus (HBV) in a mouse model for HBV replication[83]. Most SNALP targeted genes, in clinical trials, are disease-relevant targets in the liver because of theirs effectiveness in delivering nucleic acids into hepatocytes[39]. A second generation of SNALPs, ALN-TTR02 (Alnylam Pharmaceuticals), termed as Patisiran, features a DLinDMA analogue that has showed a tenfold increase in efficacy in preclinical studies, and is being evaluated for the treatment of transthyretin-mediated amyloidosis (ATTR) (NCT01960348)[84].

Several approaches have been developed to improve liposomes stability in different environments. In case of gene delivery through oral administration, some strategies as Nimos (nanoparticles in microsphere oral system) raised some interest. Nimos consists in a pDNA-based nanoparticle encapsulated within poly(epsilon-caprolactone) (PCL) microparticles. PCLs are degraded by intestinal lipases releasing the nanoparticles in the intestine and allowing them to be available for cell uptake[85].

8. Monoolein-based nanocarriers as promising vectors for small interference RNA delivery

MO (Monolein) was first proposed as a helper lipid, for non-viral pDNA delivery, in a novel liposomal formulation with the synthetic surfactant Dioctadecyl dimethylammonium bromide (DODAB)[86]. In this work, a liposomal formulation composed by DODAB and MO with different molar fractions was used to complex pDNA,

forming lipoplexes that effectively transfected Human Embryonic Kidney 293T cells, without inducing significant toxicity[87,88].

DODAB is a cationic lipid, firstly synthesized by Kunitake and Okahata in 1997[89], comprised by a quaternary ammonium headgroup (possessing one single positive charge) linked to a double acyl chain (C18:0) which tends to form LUVs in excess of water. DODAB's phase behavior has been extensively studied and its physicochemical characteristics are easily controlled, making it easy to design DODAB-based formulations with specific molecular structures. However, DODAB possesses a relatively high gel-to-liquid crystalline phase transition temperature (T_m= 45 °C)[90] that is superior to the human physiological temperature. Therefore, DODAB's bilayer displays a strong rigidity at normal body temperature limiting its use as a gene delivery system. MO is a natural-occurring neutral surfactant, possessing a single unsaturated acyl chain (C 18:1) attached to a glycerol headgroup, that forms two inverted bicountinuous cubic phases (Q_{II}^D and Q_{II}^G) in excess of water[91]. Similarly to the hexagonal structures, these cubic structures are also known to mediate membrane fusion processes[92].

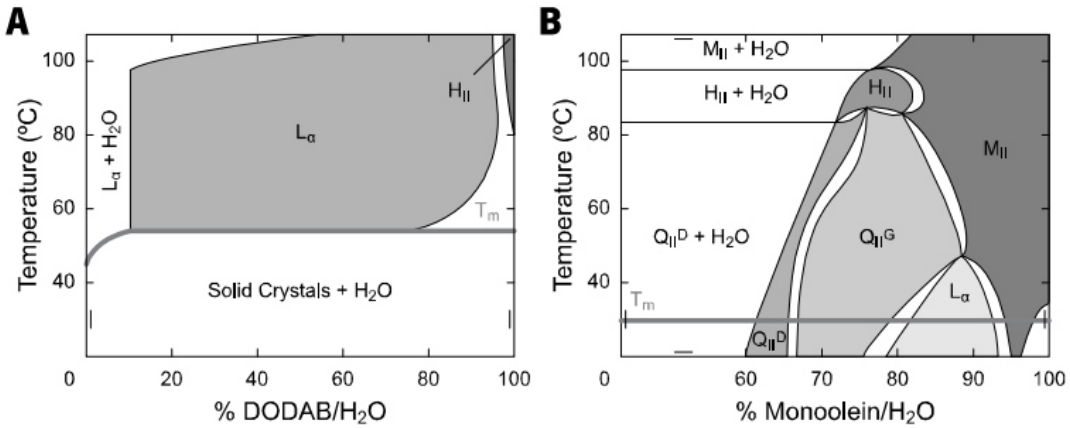

Figure 5. Lipid phase diagrams of DODAB (A) and MO (B). Liquid-crystalline lamellar (L_α), inverted hexagonal (H_{II}), inverted micellar (M_{II}) and inverted bicontinous cubic (Q_{II}^D and Q_{II}^G) (Diamond/Gyroid) phases. Adapted from[91,93].

The inclusion of a co-lipid with lower T_m, such as DOPE, cholesterol or MO, in the liposomal formulation, will lower the T_m of the lipid mixture, fluidizing DODAB's bilayer. The aggregation behavior of concentrated DODAB/MO mixtures reveals the formation of the inverted nonlamellar phases, in excess of MO, and the prevalence of a lamellar organization for MO fractions below 50 % (Figure 6)[94].

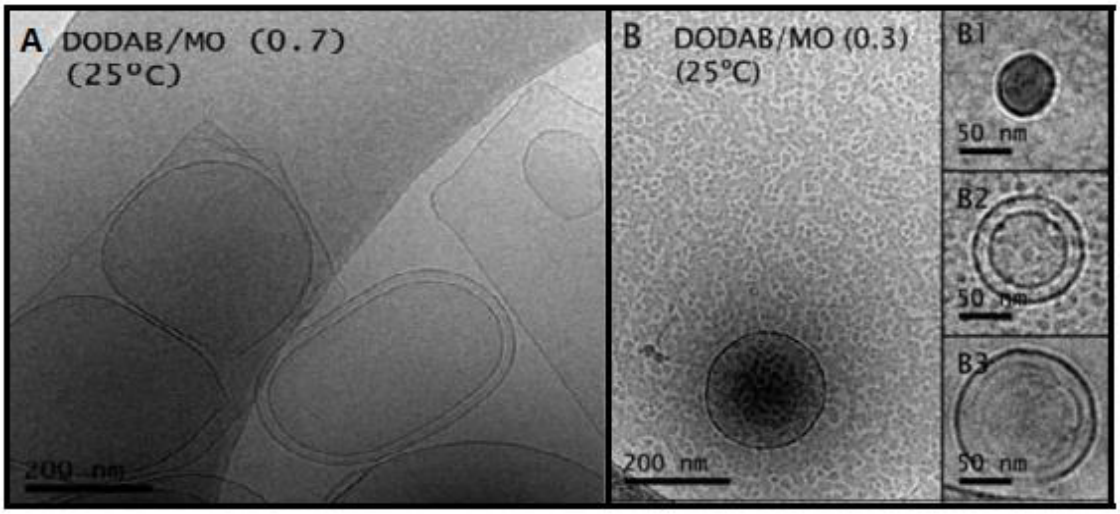

Figure 6. Cryo-TEM micrographs of DODAB:MO suspensions at χ_{DODAB}>0,5 (A) and χ_{DODAB} <0,5 (B, B1, B2, B3) at 25 °C. Scale bars: 200 nm (A,B) and 50 nm (B1, B2, B3). Adapted from[94].

The positively charged component of the liposomal formulation plays an important role in transfection efficiency of the delivery systems[33,95]. Despite the DODAB and dioctadecyldimethylammonium chloride (DODAC) molecules only differ in the counterion (Br^- and Cl^-), its effect on bilayer hydration significantly influences several properties, like the mean size and the gel to-liquid crystalline transition temperature[96-98]. Recently, Oliveira *et al*, 2014, reported the efficiency of DODAX:MO (DODAB/C:MO) nanocarriers in siRNA delivery[99]. Varying the proportion of DODAX to MO and changing the counterion from Cl^- to Br^-, altered the nanocarriers properties in such a way that not only resulted in different levels of organization (Figure 7), but also in internalization and different transfection efficiencies which, in turn, resulted in different gene silencing capability.

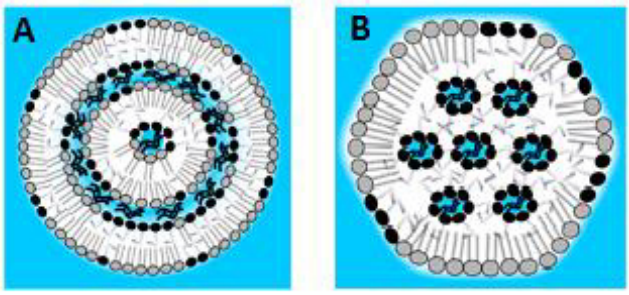

Figure 7. Schematic representation of siRNA- DODAX:MO (2:1) (A) and siRNA- DODAX:MO (1:2) (B) lipoplexes structural model. Adapted from[99].

As described before for DODAB or MO rich domains, it was hypothesized that lamellar liposomes are prevalent in DODAX-enriched formulations (DODAX:MO (2:1)),

so then the encapsulation of siRNA would maintain the lamellar phase, and a multilamellar structure will predominantly be formed with anionic nucleic acids sandwiched between the lipid membranes. For MO-enriched formulations (DODAX:MO (1:2)), where a coexistence of lamellar and nonlamellar aggregates was observed, the encapsulation of siRNA will originate a DODAX lamellar phase enclosing the MO nonlamellar phases, where the siRNA will preferentially localize. The authors also suggested that endocytosis is the main internalization route for MO-based nanocarriers. In the case of siRNA delivery, DODAB:MO-based delivery system was more efficient then the DODAC:MO-based one, promoting lower cytotoxicity, higher internalization and gene silencing in H1299 eGFP cells[99].

The major disadvantage related with the use of cationic liposomes (CL)–DNA/siRNA complexes (lipoplexes) is their low transfection efficiency. It has been reported that depending on the mode of cellular uptake, lipoplexes may be eliminated by lysosomal degradation or digestion, recycled back to the membrane, or delivered to other compartments. The use of cholesterol in the lipoplex formulation has been shown to enhance transfection both *in vitro* and *in vivo*[100,101]. Odete Gonçalves (2012), developed a DODAX:MO-based liposomal formulation including different contents of the cationic cholesterol 3β [N-(N',N'- dimethylaminoethane)carbamoyl cholesterol (DC-Chol). Depending on the preparation method, the increment of the DC-Chol has different effects on the transfection efficiency of MO-based lipoplexes but, in general terms, the presence of DC-Chol enhances the efficiency of pDNA delivery by the MO-based nanocarriers[102].

Additional research, carried out by our group, demonstrated that pegylation of the lipoplexes makes them more stable, biocompatible and suitable for siRNA delivery (unpublished results). Moreover, the coating of the delivery systems with PEG-Folate resulted in higher cellular association in folate receptor positive MDA-MB-568 cells when compared to the cellular association observed in folate negative cell line MDA-MB-435, with the nanocarriers including PEG-Folate. These results are an indicative of folate receptor-mediated internalization[103].

9. Rationale and aims

BRAF has been established by Preto *et al*, as a good target for individuals with sporadic MSI colorectal cancer harboring $BRAF^{V600E}$, thus specific target inhibition of the BRAF protein could be a promising therapeutic approach for CRC. To the best of our knowledge, no BRAF specific drug has been developed. Gene therapy, through RNAi machinery, is a reliable alternative to the conventional cytotoxic drugs used currently in a combination regime in CRC treatment. The fundamental challenge of siRNA therapy remains the development of safe, effective and specific delivery vectors. Cancer cells are known to overexpress folate receptor at the surface what constitute a good target for the development of specific nanoparticles. Attractive vehicles to deliver siRNA into target cells are the cationic liposomes because of the simplicity of their complexation with siRNAs, low toxicity and immunogenicity and superior pharmacokinetic properties and good transfection (especially if composition contains transfection enhancer like cholesterol). Elisabete Oliveira's group has established MO-based nanocarriers as promising nanocarriers for siRNA and DNA delivery.

The aim of this thesis was to develop and characterize novel DODAX:MO-based systems incorporating DC-Chol, PEG-Ceramide and PEG-Folate for specificity, in order to avoid aggregation, immune recognition and increase the transfection efficiency, for specific delivery of BRAF-siRNA in colorectal cancer cells for intravenous or local administration. To achieve our goals we tested the produced nanoparticles in RKO cell line, which is a colorectal cancer cell line harboring a $BRAF^{V600E}$ mutation.

Specifically in the project we aimed to:

1- Study the physicochemical and biophysical characteristics of DODAX:MO:DC-Chol nanocarriers.
2- Perform preliminary studies of the nanocarriers for possible routes of administration, both local and intravenous administration.
3- Validate biologically the DODAX:MO:DC-Chol nanocarriers, performing cytotoxic and cellular uptake assays.
4- Evaluate BRAF expression silencing upon transfection with by DODAX:MO:DC-Chol- BRAF siRNA nanocarriers.

II. Material and Methods

1. Reagents

The reagents dioctadecyldimethylammonium bromide (DODAB) and Ddioctadecyldimethylammonium chloride (DODAC) were purchased from Tokyo Kasei (Japan). 3ß-[N-(N',N'-dimethylaminoethane)-carbamoyl] cholesterol hydrochloride (DC-Chol), Poly(ethylene glycol)$_{2000}$C(8)ceramide (PEG-cer), 1,2-Dioleoyl-*sn*-glycero-3-phospho-L-serine (DOPS), 1,2-dioleoyl-*sn*-glycero-3-phosphatidylethanolamine-7-nitrobenzofurazan (NBD-PE) (λ_{exc} = 465 nm; λ_{em} = 535 nm) and 1,2-dioleoyl-*sn*-glycero-3-phosphoethanolamine-N-(lissamine Rhodamine B sulfonyl) (Rhodamine-PE) (λ_{exc} = 560 nm; λ_{em} = 583 nm) were purchased from Avanti Polar Lipids (Alabaster, AL, USA). The Nucleopore Track-Etch Membranes were supplied from Whatman (Maidstone, UK). The 1-monooleoyl-*rac*-glycerol (MO), HEPES buffer, Trypsin, Sulforhodamine B sodium salt (SRB) and Thiazolyl Blue Tetrazolium Bromide (MTT) reagent were purchased from Sigma-Aldrich (Bornem, Belgium). RiboGreen reagent and Lipofectamine® 2000 were supplied from Invitrogen (UK). 1,2-Dioleoyl-*sn*-glycero-3-phosphocholine (DOPC) was purchased from Corden Pharma (Liestal, Switzerland) and 1,2-dioleyl-3-phosphatidylethanolamine (DOPE) was obtained from Lipoid GMBH (Ludwigshafen, Germany). Opti-MEM I Reduced Serum Medium and Fetal Bovine Serum (FBS) were purchased from Gibco (UK). The Dulbecco's Modified Eagle's Medium (DMEM), Penicillin−streptomycin (5000 IU/mL penicillin and 5000 µg/mL streptomycin) and Hank's Balanced Salt Solution (HBSS) were supplied by Biowest (Nuaillé, France). TaqMan® Gene Assay HS01635040_S1, TaqMan® Universal Master Mix II, and TaqMan® MATP-6 and GAPDH endogenous control were supplied by Life Technologies (Carlsbad, CA, Estados Unidos). The SV Total RNA Isolation System was supplied by Promega (Madison, USA) and iScript cDNA synthesis kit was purchased by BioRad (Hercules, CA, USA). The mimicking colon fluid was gently assigned by biological engineering laboratory.

A scramble siRNA sequence (5'GUCUCAAGUUUUCGGGAAGdTdT3') was used in biophysical experiments, while, in transfections experiment, a siRNA sequence targeting human BRAF[17] was used, 5'-AAAGAAUUGGAUCUGGAUCAU-3´, both purchased by IDT (Leuven, Belgium).

2. Preparation of DODAX:MO:DC-Chol liposomes

Cationic liposomes composed of DODAX:MO:DC-Chol liposomes (2:1:0; 5:4:1; 4:1:1) (mol:mol) (Table 2) were prepared by thin lipid film hydration method followed by extrusion, as published before[99]. Briefly, defined volumes from stock solutions of DODAB or DODAC, MO and DC-Chol in ethanol (20 mM) were placed in a round-bottomed flask, and the solvent was evaporated under vacuum (15 min at 50 °C) in a rotatory evaporator (VV Micro Rotary Evaporator, Heidolf). Subsequently, the lipid film was hydrated above the melting temperature of the cationic lipids (> 50 °C), with an appropriated volume of HEPES buffer (25 mM, pH 7.4) in order to obtain a 3 mM liposomal dispersion. In order to obtain a homogenous population of unilamellar vesicles, the liposomal dispersion was subjected to 5 extrusion cycles. During this process the liposomal dispersion was forced to pass, by compression with air, first through a filter with a pore size of 400 nm (first cycle) and then four times through a 100 nm pore sized filter (Track-Etched Membranes (Nuclepore)). To increase the fluidity and facilitate the extrusion, the extruder (Lipex Extruder (Northern Lipids)) was pre-heated at 60 °C.

For the biological assays, liposomes were additionally sterilized using a membrane filter with a pore of 200 nm (Filtropur S 0.2 (Sarstedt)).

DODAX:MO:DC-Chol liposomes were post-pegylated by the addition of 10 % of PEG-ceramide (chain 8) (mol:mol) to the liposomal dispersion, followed by 1 h of incubation at 55 °C. The formulations were left to stabilize at least 20 min at room temperature before use[104].

Table 2 Lipid Molar fraction (χ) of the liposomal formulations

	X_{DODAX}	X_{MO}	$X_{DC\text{-}CHOL}$
2:1:0	0.67	0.33	-
4:1:1	0.68	0.16	0.16
5:4:1	0.50	0.40	0.10

3. Lipid mixing/Fusion assay

Förster Resonance Energy Transfer (FRET) is a non-radiative transfer of energy between an excited donor and appropriate acceptor chromophore, mediated by long-

range dipole-dipole interactions (Förster). The energy transfer requires a spectral overlap between the donor emission and acceptor absorption spectra and a minimal distance between the donor and the acceptor (lower than 10 nm). Also, the energy transfer depends on the donor and acceptor fluorescence quantum yields and the relative orientation of their transition dipole moments[105]. The energy transfer efficiency (φ_{FRET}) between donor and acceptor can be an indication of lipid mixing/fusion occurrence. Lipid probes like NBD-PE and Rho-DOPE can be used to monitor the process of lipid mixing/fusion between liposomes[106]. For instance, endosomes models labeled with these two probes can be mixed with DODAX:MO:DC-Chol liposomes, and the FRET efficiency can be determined in order to evaluate the lipid mixing/fusion processes between them.

In case of fusion or lipid mixing, an increase of the average distance between the donor and acceptor chromophores will occur, resulting in an increase of the average donor signal and in a loss of the acceptor signal, consequently decreasing the φ_{FRET}. A representation of FRET dynamics using this donor/acceptor fluorescent pair is shown in Figure 8.

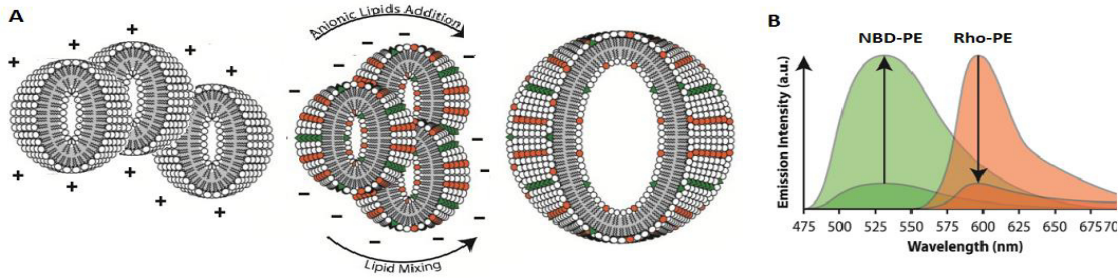

Figure 8. Theoretical model for the lipid mixing between DODAX:MO:DC-Chol and NDB-PE and Rhodamine-PE labeled endosomes models (A) and the resulting variation in donor and acceptor emission spectra (B).

Labeled liposomes composed by PC:PE:PS:Cholesterol (5:1:1:2) (mol:mol) were used as model endosomes and prepared by ethanol injection as described elsewhere[87]. The double-labeled Donor/Acceptor (DA) model endosomes included 1 % mol of NBD-PE and 2 % mol of Rho-PE, and single-labeled Donor (D) liposomes included only 1 % NBD-PE. The lipids were mixed and injected, drop by drop, in pre-warmed MES-HEPES buffer (20 mM, pH 7.2 and/or pH 5.5) under strong vortex stirring and let to stabilize at room temperature. The pH 7.2 and/or pH 5.5 were used in order to mimic early and late

endosomes model. To perform the fusion assay, 50 µM of the (DA) or (D) early or late endosomes model, and 50 µM of the DODAX:MO:DC-Chol liposomes were mixed and the final volume was raised to 2.5 mL with MES-HEPES buffer (pH 5.5 or 7.2). The fluorescence emission spectra (480 - 700 nm) was recorded in a Luminescence Spectrometer LS 50 (Perkin-Elmer) using a λ_{exc} = 460 nm, with spectral bandwidths of 1 nm. The steady-state φ_{FRET} of the liposomes containing both donor and acceptor fluorophors as determined according to following equation:

Equation 1. ϕ_{FRET} equation

$$\phi_{FRET}\,(\%) = \frac{F_D - F_{DA}}{F_D} \times\ 100$$

where F_D is fluorescence intensity of the single-labeled liposomes and F_{DA} is fluorescence intensity of the double-labeled liposomes at λ_{em} = 530 nm. FRET was quantified as a function of time after addition of DODAX:MO:DC-Chol liposomes to the (D) and (DA) endosomes model.

4. Preparation of siRNA-based DODAX:MO:DC-Chol lipoplexes

siRNA-lipoplexes were prepared by incubating 100 µL of siRNA solution (4 µM) in HEPES buffer (25 mM, pH 7.4) with appropriated volumes, in order to obtain the desired charge ratios, of DODAX:MO:DC-Chol liposomes (1 mM), prepared according to section 3. After vortex stirring, the lipoplexes were left 20 min at room temperature. The balance between charges is given by the charge ratio (+/-).

Equation 2. Charge ratio calculation

$$C.R.(+/-) = \frac{[+]}{[-]} = \frac{[Ammonium\ groups\ of\ DODAX + Amine\ groups\ of\ DC - Chol]}{[Phosphate\ groups\ from\ siRNA]}$$

The positive charges are given by the concentration of ammonium groups present in DODAX lipids and by the amine present in DC-Chol, where the negative charges are given by the number of phosphate groups in siRNA, which is directly correlated with the nucleotide concentration.

Post-pegylated siRNA-lipoplexes were prepared through the addition of 10 % of PEG-ceramide (chain 8) to the cationic lipid presented in solution (mol:mol), followed by

1 h of incubation at 55 °C as described before. The formulations were let to stabilize at least 20 min at room temperature before use.

5. RyboGreen assay

Non-pegylated siRNA-DODAX:MO:DC-Cholesterol lipoplexes were prepared at charge ratios (+/-) 1, 3, 5, 7, 10 and 15, as described above. Efficiency of siRNA encapsulation was characterized by RiboGreen assay. RiboGreen is a RNA intercalating fluorescence probe used to quantify RNA in solution.

The RiboGreen assay was performed according manufacturer specifications: 100 µL of lipoplexes, HEPES buffer (25 mM, pH 7.4) as blanck, and siRNA (0.4 µM) (the concentration of siRNA in diluted lipoplexes) were plated in a dark 96 well plate (NUNC, Denmark). Then, 100 µL of RiboGreen (200x) was added to each condition and incubated for 5 min in the dark. The fluorescence was measured in a Fluoroskan ACEN FL Microplate Fluorometer and Luminometer (Thermo scientific), using the excitation/emission filter pair of 485/538 nm. The RiboGreen solution was prepared by 200x fold dilution of the RiboGreen stock solution (750 mM) in a Tris-EDTA buffer (10 mM Tris-HCl, 1 mM EDTA, pH 7.5) (200x) diluted from the stock solution with ultrapure water RNase free. All procedure was carried on ice and using RNAse free material.

6. Size and Zeta-potential measurements

7.1 Dynamic light scattering (DLS) assay

Dynamic light scattering, or photon correlation spectroscopy technique, is based on thermally induced particles collisions with the solvent molecules, resulting in the spontaneous diffusion towards a homogeneous distribution on solvent, known as Brownian motion. The particle movement is inversely proportional to particle size: the smaller the particles are, the more rapidly they move, as portrayed in stokes-Einstein equation.

Equation 3. Stokes-Einstein Equation

$$D = \frac{k_B T}{6\pi\eta R_H}$$

where (D) is the diffusion coefficient of the particle, (k_B) the Boltzmann constant (1.38 x 10^{-23} $m^2kg\ s^{-2}K^{-1}$), (T) the temperature, (η) the dynamic viscosity of the dispersion medium and (R_H) is the hydrodynamic radius of the particle.

The intensity of the detected scattered light fluctuates over time (t) at a rate that is particle size dependent. The parameters obtained through cumulative analysis, are the Z-average size and the of polydispersity index (PdI), according to equation:

Equation 4. Polynomial fit to the log of the of the scattered light fluctuation in time.

$$Ln\ (G1) = a + bt + ct^2 + dt^4 + et^4 + \ldots$$

The parameter *b* is known as the z-average diffusion coefficient, and is converted to size using the dispersant viscosity, and some other instrumental constants, and the polydispersity index ($2c/b^2$). The z-average parameter is only reliable when PdI is lower than 0.1, above this, z-average can only be used for comparisons purposes (Malvern 2004). When the size distribution is very broad, the polydispersity will be too high (> 0.5) and the calculated z-average value will be unreliable. In this case, the distribution analysis should be used instead of the z-average value[107].

For size measurements, DODAX:MO:DC-Chol liposome were diluted in HEPES buffer (25 mM, pH 7.4) to a final volume of 1 mL and final lipid concentration of 1 mM. Measurements were performed in disposable polystyrene cuvettes (Sarstedt, Germany), at 25 °C, in a Malvern ZetaSizer Nano ZS particle analyzer (Malvern Instruments, UK).

Total complexation between liposomes and siRNA occurs when the efficiency of siRNA encapsulation is similar to 100 %, and hydrodynamic radius of the lipoplexes is similar to the liposomes. Therefore, non-pegylated and post-pegylated lipoplexes, prepared at charge ratio 7, were also characterized by dynamic light scattering using a similar processing protocol used for the liposomes processing.

7.2 Electrophoretic light scattering (Zeta (ζ-) potential) assay

Electrophoretic light scattering is a quasi-elastic light scattering technique that measures the surface charge of particles in a solvent, through the ζ- potential. Charged

colloidal particles are characterized by two layers around their surface that result from attracted counter-ions: a Stern layer formed by counter-ions firmly attached, and an external diffuse layer characterized by a dynamic equilibrium between positive and negative ions, being either attracted or repelled by the Stern layer or other ions.

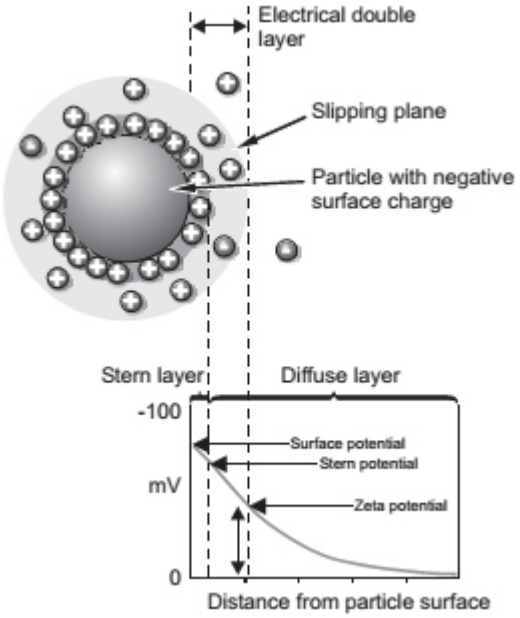

Figure 9. Schematic representation of the electrical double layer surrounding a particle in suspension, with the correspondent potential to each component of the layer[107].

Zeta potential is the electric potential resulting from the electrical double layer, and can be measured through an electrical field application. When an electric field of know strength is applied to particle dispersion, it produces a particle movement known as electrophoretic mobility. The relation between the electrophoretic mobility (μ) of a particle and its corresponding zeta potential (ζ) is given by the Henry's equation.

Equation 5. Henry's Equation

$$\mu = \frac{\varepsilon_r \varepsilon_0 \zeta}{\eta} f_H(Ka)$$

where (ε) is the dielectric constant of the dispersion medium, (η) the viscosity of the dispersion medium, and f_H(ka) is the Henry's function that correlates the ratio of the particles radius to the double layer thickness. ζ-potential measurements also provide information about the stability of the particle dispersion: high zeta potential values (superior to +30 or inferior to -30 mV) mean that electrostatic repulsions overcome the

Van der Wall interactions, thus preventing particle aggregation. Oppositely, neutral zeta potential values can contribute for particle aggregation[108].

For ζ-potential measurements, DODAX:MO:DC-Chol liposomes and lipoplexes, were processed in a similar way as for size measurements, however, using folded capillary cells (Malvern). Measurements were performed in (Sarstedt, Germany), at 25 °C, in a Malvern ZetaSizer Nano ZS particle analyzer (Malvern Instruments, UK).

Total complexation between liposomes and siRNA occurs when the efficiency of siRNA encapsulation is similar to 100 %, whereas the lipoplexes charge surface is similar to liposomes. Therefore, the ζ -potential of lipoplexes and post-pegylated lipoplexes, prepared at charge ratio (+/-) 7, were evaluated.

7. Cell lines and culture conditions

The RKO cell line is a poorly differentiated colorectal cancer cell line harboring a $BRAF^{V600E}$ mutation[109].The cell line was grown in DMEM supplemented with 10 % (v/v) of heat-inactivated FBS and 1 % (v/v) of an antibiotic/antimycotic (Penicillin−streptomycin) solution. RKO cell line was maintained at 37 °C and 5 % CO_2 in a humidified incubator and routinely passaged every 3 or 4 days using 0.05 % Trypsin-EDTA solution in order to maintain subconfluency.

8. Hemolysis assay

Hemocompatible nanocarriers can be defined as nanoparticles which do not induce any form of toxicity and remain efficacious after being exposed to blood. Hemolysis assays are one of the regularly conducted tests when evaluating the hemocompatibility of new nanoformulations.

The hemolytic activity of liposomes was investigated using an established method based on the release of hemoglobin from damaged erythrocytes. Briefly, erythrocytes were isolated from 5 mL of fresh blood by centrifugation (600 g, 10 min). The erythrocytes were washed in PBS until the supernatant was clear and colorless and then diluted to the original volume of 5 mL. 150 µL aliquots of the erythrocyte suspension were incubated with 150 µL of DODAX:MO:DC-Chol liposomes for 30 min at 37 °C in a water bath, as described elsewhere[110]. For this experiment, liposomes were diluted in pure PBS buffer (pH 7.4) and added in order to achieve final concentrations of 5, 25 and

50 µg/mL in 300 µL of total volume. After a centrifugation at 600 g for 10 min, to pellet the erythrocytes, the hemoglobin concentration in the supernatant was quantified measuring the absorbance at 541 nm, using a SpectraMax Plus 384 absorbance Plate Reader (Molecular Devices). A 2 % triton X-100 solution and H_2O were used as the positive control and PBS buffer (pH 7.4) as negative control. PBS was used as blank.

The percentage of hemolysis was quantified using the following equation:

Equation 6. Hemolysis Equation

$$\%\, Hemolysis = \frac{Abs_{sample} - Abs_{blank}}{Abs_{positive\ control} - Abs_{blank}}$$

9. Cytotoxic assays

The cytotoxicity of the pegylated and non-pegylated DODAX:MO:DC-Chol liposomes was assessed in the RKO cell line by MTT and sulforhodamine B assays.

Briefly, after reaching the exponential phase of growth, RKO cells were seeded at 7500 cells per well, in 96 well plates (TPP, Switzerland) and left 12-24 h, for adhesion, in an atmosphere of 5 % CO_2 and at 37 °C. After cell culture medium removal, the cells were incubated with non-pegylated and pegylated liposomes, diluted in DME medium to final concentrations of 5, 25 and 50 µg/mL. DMEM medium was used as a viability control and DMSO at 30 % (v/v) as a cell death control. Additionally, an appropriated quantity of HEPES buffer (25 mM, pH 7.4) was used as a control mimicking the higher quantity of liposome added and a blank control of solvent. The cells were maintained in proper culture conditions for 48 hours, at 37 °C with 5 % CO_2 and then subjected to cytotoxicity assays.

10.1 MTT assay

The MTT (3-[4,5-dimethylthiazol-2-yl]-2,5 diphenyl tetrazolium bromide) assay is based on the conversion of MTT into formazan crystals by metabolically active cells. This tetrazolium salt is metabolized by mitochondrial enzymes, resulting in a colorimetric product that can be quantified by absorption at 570 nm. In case of metabolism failure, the formazan crystals will be blocked resulting in a decrease on absorption light. The assay determines the total mitochondrial activity, a measurement of metabolic activity

that is related to the number of viable cells[111]. MTT assay is widely used to measure the *in vitro* cytotoxic effects. The cytotoxicity of the liposomes was assessed in the RKO cell line by the MTT assay, after 48 h incubation

Briefly, after incubation period, 10 µL of a MTT stock solution (5 µg/mL in PBS 1x) was added to the cells, followed by a period of 4 h of incubation, in humidified incubator (37 °C, 5 % CO_2). Finally, 110 µL of a solubilization solution, composed by isopropanol with 1 % of HCl (37 %) and 10 % of Triton X-100, was added to each well and the formazan crystal were dissolved by resuspension with the multi-channel pipette. The absorbance was measured at 570 nm in a SpectraMax Plus 384 absorbance Plate Reader (Molecular Devices) using the appropriated software (SOFT Max Pro) protocol, and the absorbance at 690 nm was also determined as a reference value.

10.2 Sulforhodamine B colorimetric assay

Sulforhodamine B (SRB) assay is a colorimetric experiment based on protein staining. The SRB dye binds to basic amino acids of cellular proteins and then colorimetric evaluation provides an estimate of total protein mass which is related to cell number, consequently a measure of cytotoxicity[112].

After an incubation period, the cell culture medium was removed, the cells were washed with PBS 1x, and 250 µL of 1 % acid acetic in methanol (100 %) solution was added to the wells. The plates were incubated at -20 °C for 1 h and 30 min and then left to dry in an incubator at 37 °C for 15 min. Afterwards, 50 µL 0.5 % Sulforhodamine B (in 1 % acid acetic) was added to each well, and the plates were incubated for 1 h and 30 min at 37 °C in the dark. In order to remove the unbound SRB, the wells were washed with 1 % acid acetic solution, and left to dry at 37 °C for 10-15 min. Finally, 100 µL of Tris 10 mM was used to dissolve SRB, and the absorbance was read at 540 nm in SpectraMax Plus 384 absorbance Plate Reader (Molecular Devices) using the appropriated software (SOFT Max Pro) protocol.

10. Cellular uptake assay

In cellular uptake experiment, liposomal formulations were prepared, with 2 mol % of NBD-PE, by the film hydration method followed by extrusion and post-pegylation. After reaching the exponential phase of growth, RKO cells were seeded at a density of 3.2 x10^4 cells per well in 24 well plates (TPP, Switzerland). After 30 min of incubation at

4 °C, the cells were washed two times with PBS 1x, treated with 25 and 50 µg/mL of the liposomal formulations (diluted in HBSS) and incubated for 6 h at 37 °C, 5 % CO_2. Then, the extracellular medium was aspirated and the cells were washed with cold PBS 1x in order to remove extracellular fluorescence residues. The cells were finally lysed with 500 µL of Triton X -100 (5 % Triton X-100 in PBS) and collected for fluorescence measurements. The internalized lipid concentration was inferred from calibration curves, obtained performing appropriated dilutions of the liposomal dispersions in Triton X -100 (5 % Triton X-100 in PBS). The fluorescence measurements were performed in a SynergyMx with Gen5TM software (Bio-Tek Instruments, Inc., EUA), using the excitation/emission filter pair of 580/530 nm. A 1 % triton X-100 solution and H_2O were used as the positive control and PBS buffer (pH 7.4) as negative control.

11. BRAF silencing by RNA interference using nanocarriers

12.1 Transfection of BRAF small interference RNA

RKO cells were transfected 24 h after seeding at 6.2 x 10^4 in 12-well plates (final volume of 1 mL/well). Cells were washed with PBS 1x and incubated with 750 µL of Opti-MEM (Reduced serum medium). Pegylated and non-pegylated DODAB:MO:DC-Chol lipoplexes (5:4:1; 4:1:1) were prepared according with section 4. 250 µL of 100 nM of the lipoplex (DODAB-based lipoplexes and pegylated DODAB-based lipoplexes) diluted in Opti-MEM (final volume 1 mL/well) were added to each well. Control cells were transfected with 3 µL lipofectamine® 2000 and 100 nM of BRAF siRNA, according to the manufacturer instructions. Briefly, 3 µL lipofectamine 2000 (Invitrogen) was diluted in Opti-MEM at a final volume of 125 µL (Mix I) and incubated 5 min at room temperature (RT). Then, 5 µL of BRAF were diluted in Opti-MEM at a final volume of 125 µL (Mix II). Mix I and II were gently combined, followed by an incubation period of 20 min at RT and then added to control well. Cells were incubated for 14 h at 37 °C, then the medium growth was refreshed and the cells were incubated for 48 h at 37 °C. All procedures were performed under RNAse free conditions and forward transfection was used.

12. Quantitative Polymerase Chain Reaction assay

Quantitative Chain Reaction (qPCR) assay is based in polymerase chain reaction which is used to amplify and allows precise quantification of specific nucleic acids in a

complex mixture by fluorescent detection of labeled PCR products. Detection can be accomplished using specific as well as nonspecific fluorescent probes. qPCR is often used in the quantification of gene expression levels as it is the most sensitive technique. BRAF-siRNA silencing of DODAB:MO:DC-Chol (5:4:1; 4:1:1) was evaluated by qPCR.

RNA extraction was performed using SV Total RNA Isolation System (Promega) according manufactures protocol. Briefly, 175 µL RNA Lysis Buffer (RLA) (+ BME) was added at each well and transferred for microtubes. After, 350 µL RNA Dilution Buffer (RDA, blue) were added to each condition and mixed by inverting 3–4 times. After heating the sample at 70 °C for 3 min, they were centrifuge for 10 min at 14 000 g and the cleared lysates were transferred to fresh tubes. 200 µL of 95% ethanol were added to cleared lysate and mixed well. The solutions were transferred to Spin Basket Assembly and centrifuged for 1 min (14 000 g). After discard eluate, 600 µL of RNA Wash Solution (RWA) (+ ethanol) were added and the solution were centrifuged for 1 min (14 000 g) and the eluate were discard again. 50 µL of DNase mix (for preparation: 40 µL of Yellow Core Buffer; $MnCl_2$, 5 µL of 0.09 M; 5 µL of DNase I) were added to the membrane of the Spin Basket Assembly and incubated at RT for 15 minutes. The reaction was stopped by adding of 200 µL of DNase Stop Solution (DSA) (+ ethanol) being subjected to a centrifugation for 1 min (14 000 g). The membrane was washed by adding, firstly 600 µL and after 250 µL of RNA Wash Solution (RWA), centrifuged for 1 min and 2 min at 14 000 g, respectively. To elute RNA, 35 µL of Nuclease-Free Water were added to the membranes and centrifuged for 1 min and stored at - 80 °C. The successful of cDNA synthesis depends on RNA purity, quality and quantity (< 1 µg).

In order to evaluate extracted RNA, the quantification by absorbance was performed in a NanoDrop 1000 Spectrophotometer (Thermo Scientific). The absorbance was read at λ 260 (A260) and 280 (A280) and expressed as a ratio (A260/A280) which was used as quality reference that should be between 1.8 and 2.2. Quality control was also verified using absorbance measured at λ=230.

In order to synthetize cDNA from extracted RNA, iScript cDNA synthesis kit (BioRad) was used. To perform the cDNA synthesis, RNA template at maximum 1 µg is diluted in nuclease-free water in a final volume of 15 µL. Firstly, were added the nuclease-free water, followed by the addition of 4 µL of 5x iScript reaction mix and the determined volume of RNA template, finally 1 µL of iScript reverse transcriptase was

added in a 20 µL of total volume per reaction. All procedure were carried on ice and with RNAse-free tips. The conversion to cDNA was performed in a CFX96 Touch™ qPCR Detection System (BioRad) were carried the following reaction protocol: 5 min at 25 °C, 60 min at 42 °C, 5 min at 85 °C and held at 4 °C. The cDNA storage was performed at -20 °C.

The PCR reaction mix was proceed by adding 1 µL of 20X TaqMan Gene Expression Assay (BRAF or MT-ATP6) (Applied Biossystems), 10 µL 2X TaqMan Gene Expression Master Mix (Applied Biossystems), 1 µL cDNA template and 8 µL RNAse free water (volume for 20 µL per reaction). The qPCR was conducted in CFX96 Touch™ Real-Time PCR Detection System (BioRad) using the following protocol: 120 min at 50 °C, 10 min at 95 °C 15 sec at 95 °C and 60 min at 60 °C, repeated 50 times.

Data analysis was performed using the Comparative C_t Method, also referred as the ΔΔCt Method. Comparing samples requires normalization to compensate for differences in the amount of biological material in samples. The most current strategy is the normalization with internal reference gene (endogenous control MT-ATP6). ΔΔCt Method is applied when the primers of target and endogenous genes has a 100 % efficiency. The relative expression of the two genes, ΔCT value, is calculated by following equation:

Equation 7. ΔC_T Equation

$$\Delta C_T = C_{T\ target} - C_{T\ endogeno\ control}$$

where exponent C_T (Cycle threshold) accounts for the production of double stranded DNA in the first PCR cycle from the single stranded cDNA template generated by the reverse transcription reaction. To evaluate expression level of the determined gene relatively to the calibrator should be performed:

Equation 8. $\Delta\Delta C_T$ Equation

$$\Delta\Delta C_T = \Delta C_T\ test\ sample - \Delta C_T\ calibrator\ test$$

The amount of target, normalized to an endogenous reference and relative to a calibrator, is given by:

Equation 9. Ratio of gene expression

$$Ratio = 2^{-\Delta\Delta C_T}$$

13. Statistical Analysis

Statistical analysis was performed with GraphPad Prism 5.0 software, using the one-way ANOVA test, followed by a Dunnett's or Tukey's multiple comparison test or two-way ANOVA test, followed Bonferroni post-test. Results were expressed as mean ±standard deviation (S.D.), and $p < 0.05$ was considered to be statistically significant.

III. Results

1. Physicochemical characterization of DODAX:MO:DC-Chol liposomes

a. Hydrodynamic diameter and surface charge

Hydrodynamic diameter and surface charge of DODAX:MO:DC-Chol liposomes were determined by Dynamic Light Scattering (DLS) and Electrophoretic light scattering (ζ-potential) (Figure 10).

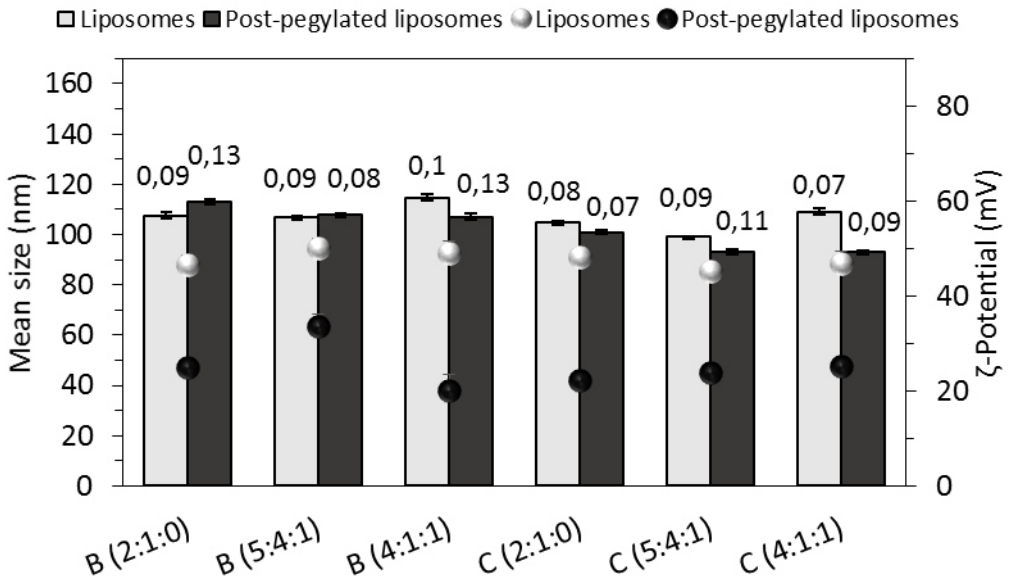

Figure 10. Z-average mean size (nm), (columns), Polydispersity Index (PdI), (values on top of the size columns), and ζ-potential (mV), (circles), of DODAB:MO:DC-Chol (B) and DODAC:MO:DC-Cho l(C) (2:1:0; 5:4:1 and 4:1:1) ratios liposomes. Data are presented as mean ± standard deviation (S.D.) obtained from two independent experiments.

DODAX:MO:DC-Chol liposomes prepared by thin lipid film hydration method, followed by extrusion, presented a uniform size distribution (PdI<0.1) with hydrodynamic diameter between 100-120 nm and were positively charged (ζ-potential>44 mV). DODAB-based liposomes had slightly higher mean size and had a more polydisperse population than DODAC-based liposomes. No significant differences were observed concerning the liposomal surface charge when comparing the two counterions. The inclusion of DC-Chol in liposomal formulations, at lower contents (10 % in the formulation 5:4:1), maintain or decreased the Z-average of DODAB and DODAC-based liposomes, respectively. At higher contents (16 % in formulation 4:1:1), DC-Chol increases both DODAB and DODAC-based liposomes mean sizes. DODAB:MO:DC-Chol

(4:1:1) and DODAC:MO:DC-Chol (4:1:1) presented the highest values of hydrodynamic diameter, 115 nm and 109 nm, respectively.

Post-pegylation maintained or decreased the mean size and the polydispersity of the liposomes (100-120 nm) (PdI<0.1), except for DODAB:MO:DC-Chol (2:1:0) formulation, where post-pegylation increased the liposomes mean size from 107.6 nm (non-pegylated) to 112.9 nm (pegylated). Pegylated DODAB-based exhibited higher mean size values compared with pegylated DODAC-based liposomes. Also, the mean size of pegylated liposomes seems to be dependent on DC-Chol content. In DODAB-based liposomes, the higher the DC-Chol content, the lowest the mean size of liposomes. Pegylated DODAC:MO:DC-Chol (5:4:1 and 4:1:1) exhibited the lowest values of mean size (93 nm) while pegylated DODAB:MO:DC-Chol (2:1:0) presented the highest mean size (113 nm).

All MO-based liposomes presented similar ζ-potential values. Moreover, higher contents of cationic lipids in DODAX:MO:DC-Chol (4:1:1) (82 % mol:mol of DODAX + DC-Chol) did not result in higher ζ-potential values when compared to the other DODAX:MO:DC-Chol dispersions.

Our data showed that the post-pegylation reduced, significantly, the liposomes surface charge (around 20 mV). No significant changes in the ζ-potential values were detected between pegylated DODAB and DODAC-based liposomes.

In pegylated DODAB-based liposomes, (5:4:1) liposomes presented the highest ζ-potential (33.5 mV), followed by (2:1:0) (24.9 mV), and then (4:1:1) (20.2 mV), while for DODAC-based liposomes the ζ-potential slightly increases with the increase of DC-Chol. DODAC:MO:DC-Chol (2:1:0) liposomes presented the highest ζ-potential (22.2 mV), followed by (5:4:1 with 10 % of DC-Chol) (23.8 mV), and then (4:1:1 with 16 % DC-Chol) (25.3 mV).

DODAB:MO:DC-Chol (5:4:1) formulation presented the highest value of surface charge (33 mV) and DODAB:MO:DC-Chol (4:1:1) the lowest value of surface charge (20 mV).

b. Stability over time of non-pegylated liposomes

The mean size and ζ-potential of the non-pegylated DODAX:MO:DC-Chol liposomes were monitored over 30 days (Figure 11).

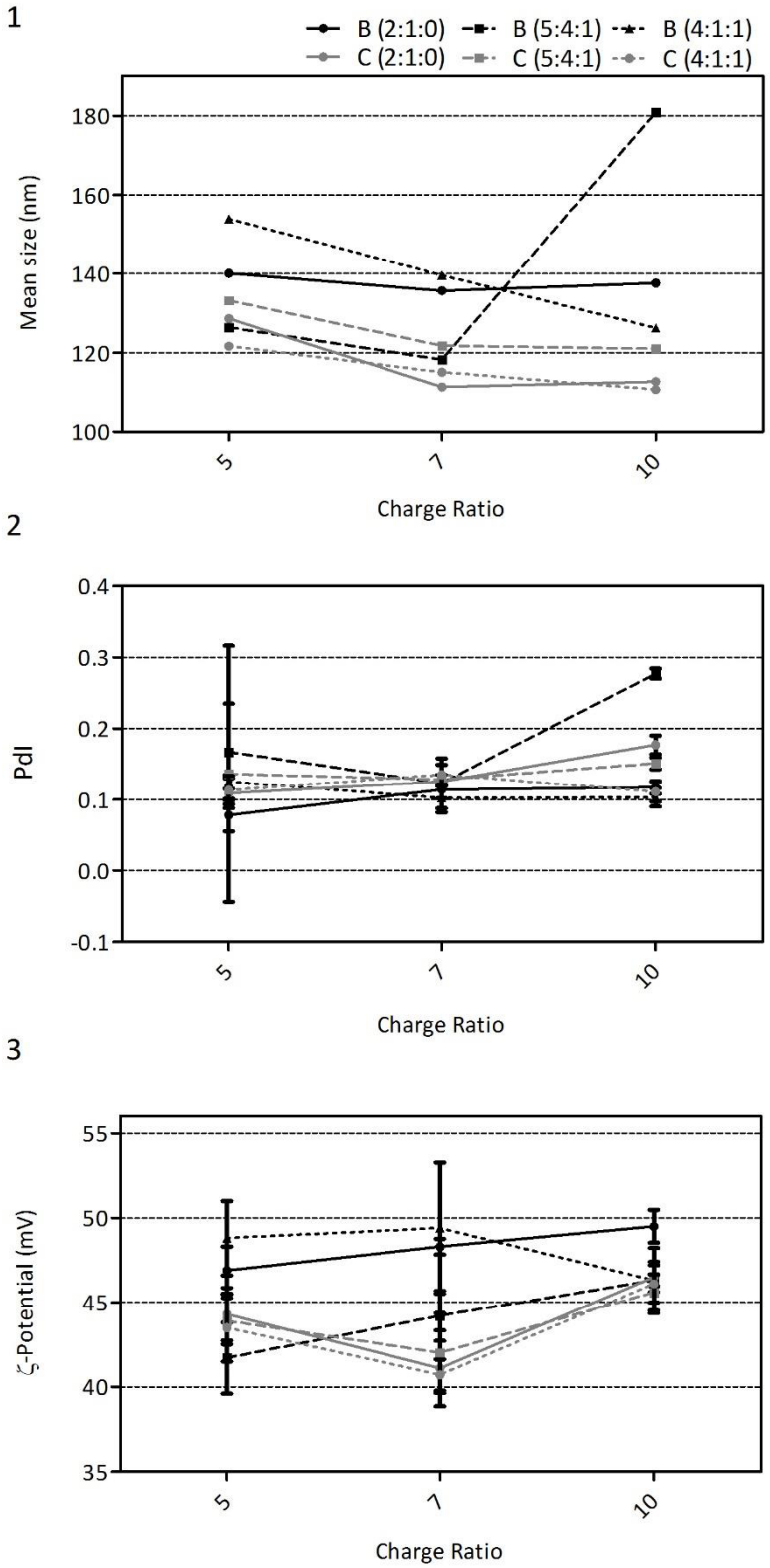

Figure 11. Stability over time of non-pegylated DODAB/C:MO:DC-Chol liposomes. Z-average mean size (nm) (1); Polydispersity Index (PdI) (2) and ζ-potential (mV) (3) of DODAB:MO:DC-Chol (B) and DODAC:MO:DC-Chol (C) liposomes over 30 days. Data are presented as mean ± S.D.

All MO-based liposomes were stable in HEPES buffer solution (pH 7.4, 25 mM) for this period of time in terms of mean size, PdI and ζ-potential.

c. Evaluation of lipid mixing/fusion ability of non-pegylated liposomes

Endosomal escape is determinant for a successful gene silencing and depends on the nanocarriers ability to destabilize/fuse with the endosome membranes. In order to mimick early and late endosomes, the fusogenic ability of DODAX:MO:DC-Chol liposomes was evaluated at neutral and acidic conditions, by Foster Resonance Transfer (FRET) assay, using the pair NBD-PE (donor) and Rho-PE (acceptor) fluorescence probes (Figure 12).

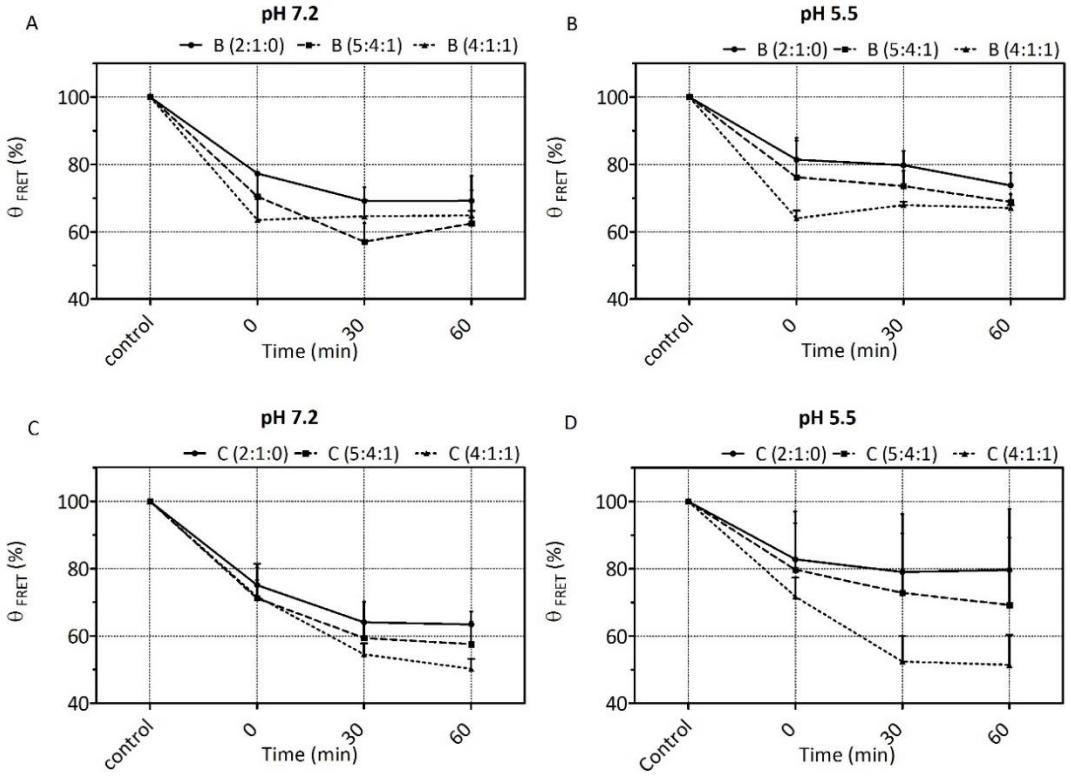

Figure 12. Ability of non-pegylated DODAX:MO:DC-Chol liposomes to destabilize model endosomal membranes, as assessed by FRET. (A) FRET efficiency (ϕFRET) after incubation of DODAB:MO:DC-Chol liposomes with model early endosomes (pH 7.2). (B) ϕFRET after incubation of DODAB:MO:DC-Chol liposomes with model late endosomes (pH 5.5). (C) ϕFRET after incubation of DODAC:MO:DC-Chol liposomes with model early endosomes (pH 7.2). (D) ϕFRET after incubation of DODAC:MO:DC-Chol liposomes with model late endosomes (pH 5.5). Control-model of early or late endosomes in the absence of DODAX:MO:DC-Chol liposomes, (DODAB:MO:DC-Chol (B) and DODAC:MO:DC-Chol (C)) corresponding to maximum Φ_{FRET}. Data are presented as mean ± S.D. obtained from two independent experiments.

All MO based liposomes exhibited a reduction in FRET signal at both pH 7.2 and pH 5.5, suggesting a lipid mixing/fusogenic ability of the nanocarriers to interact with

early/late endosomes. DODAB-based nanocarriers exhibited a similar reduction in FRET signal for both pH while DODAC-based exhibited a more pronounced reduction in acidic pH. The inclusion of DC-Chol in nanoformulation (10 % in 5:4:1 and 16 % in 4:1:1) increased lipid mixing/ fusogenic ability between nanocarriers and early/late endosomal model when compared to DODAX:MO:DC-Chol (2:1:0) liposomes. Moreover, an increase in the amount of DC-Chol from 10 % in (5:4:1) formulation to 16 % in (4:1:1) formulation resulted in a higher fusogenic capacity of the liposomes at both pH conditions. DODAB:MO.DC-Chol-based (4:1:1) nanoformulation promoted a decrease in FRET in of 34 % and in 38 % while DODAC-based liposomes (4:1:1) promoted a reduction in 50 % and in 55 % at pH 7.2 and pH 5.5. A slightly decrease on FRET over time is detected for both DODAB and DODAC-based nanocarrier, which was more pronounced in acidic conditions in case of the DODAC-based liposomes comparing with DODAB-based liposomes. The fact that the formulation DODAX:MO:DC-Chol (5:4:1) possess higher MO content (40 %) did not provide higher fusogenic capacity when compared with formulations with lower MO content (33 % in 2:1:0 and 16 % in 4:1:1 formulations).

2. Biophysical characterization of DODAX:MO:DC-Chol siRNA-lipoplexes

a. Small interference RNA encapsulation efficiency

RiboGreen assay uses a RNA intercalating fluorescence probe to quantify RNA in solution. RiboGreen assay was performed to calculate the siRNA encapsulation efficiency of MO-based liposomes. In Figure 13, it is possible to visualize the siRNA encapsulation dynamics of non-pegylated DODAX:MO:DC-Chol formulations.

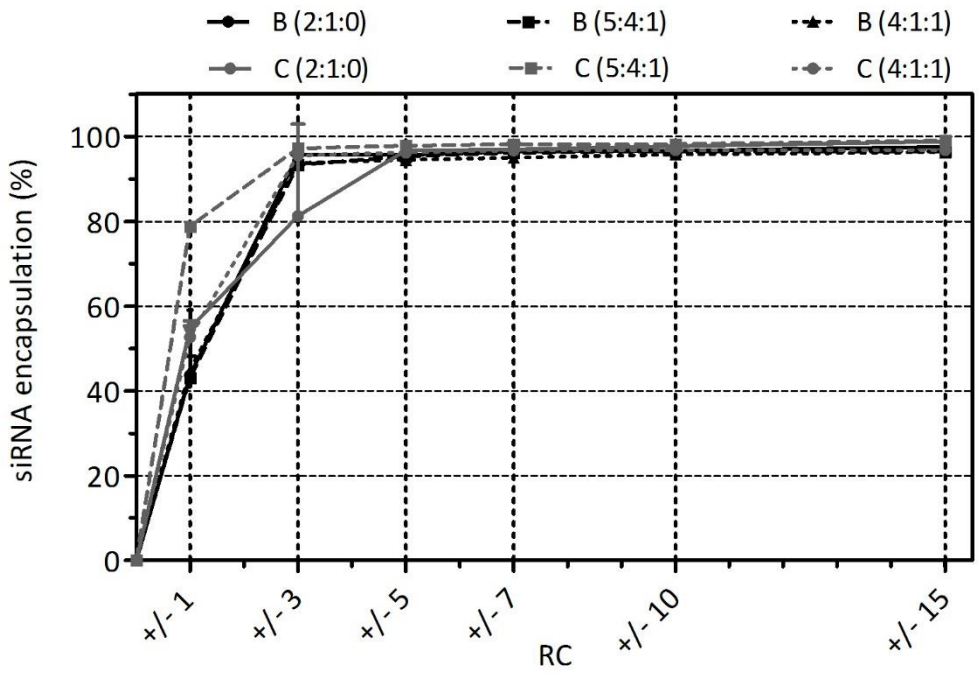

Figure 13. siRNA encapsulation efficiency by non-pegylated DODAB/C:MO:DC-Chol (DODA liposomes at different C.R.. DODAB:MO:DC-Chol (B) and DODAC:MO:DC-Chol (C). 0 % indicates the higher degree of RiboGreen intercalated in a free siRNA solution with the same siRNA concentration as used in the siRNA-lipoplexes. Data are presented as mean ± S.D. obtained from two independent experiments.

All DODAB-based formulations exhibited the same dynamics of siRNA encapsulation, independently on the lipids content. In DODAC-based liposomes, the inclusion of DC-Chol significantly improved siRNA encapsulation efficiency at lower CR (+/-) (<5), with DODAC:MO:DC-Chol (2:1:0) only reaching its maximum siRNA encapsulation at CR (+/-)5. Nevertheless, it is the lowest content of the DC-Chol (10 %) balanced with a high MO content (40 %) in DODAC:MO:DC-Chol (5:4:1) formulation, that promoted the better siRNA encapsulation efficiency when compared to all the other formulations. However, with the increase of charge ratio (+/-) (>5), all formulations presented approximately the same siRNA encapsulation efficiency (>97 %).

b. Hydrodynamic diameter and surface charge of DODAX:MO:DC-Chol siRNA-lipoplexes

In order to determine the charge ratio with the best features in terms of size, PdI and ζ-potential, Dynamic and Electrophoretic Light Scattering measurements where performed in lipoplexes prepared at the charge ratios with the highest siRNA encapsulation efficiencies, namely CR (+/-) 5,7 and 10 (supplementary material). Figure 14 revealed the physicochemical characterization of lipoplexes and post-pegylated

lipoplexes at charge ratio (+/-) 7, since at this CR we considered that maximum siRNA encapsulation was already achieved, while the excess of lipid added to siRNA was still acceptable. Moreover, we intend to avoid empty liposomes but not lacking totally particle formation.

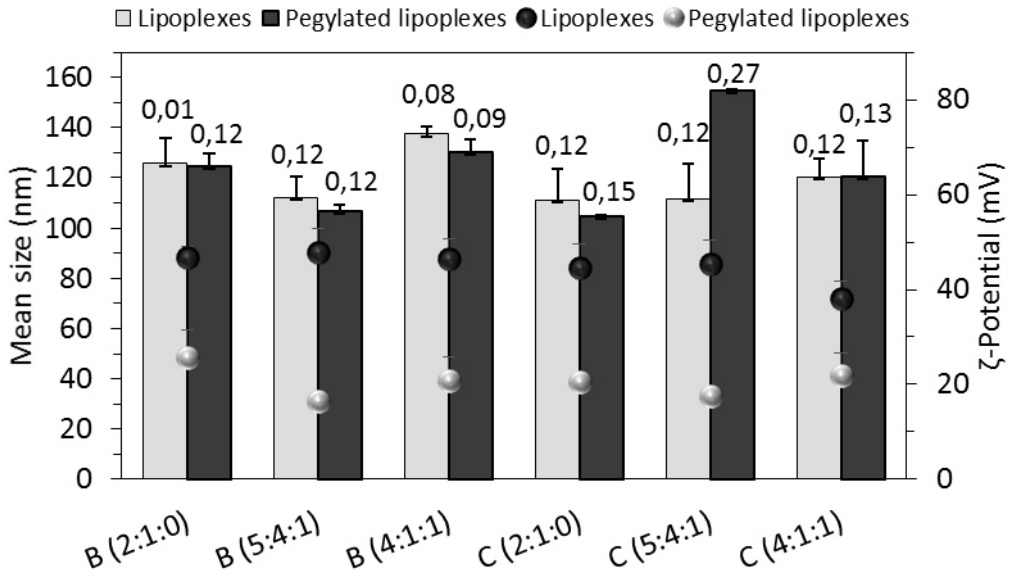

Figure 14. Z-average mean size (nm) (columns), Polydispersity Index (PdI) (value above the columns), and ζ-potential (mV) of non-pegylated (black circumferences) and post-pegylated DODAB/C:MO:DC-Chol siRNA-lipoplexes (white circumferences). DODAB:MO:DC-Chol (B) and DODAC:MO:DC-Chol (C). Data are presented as mean ± S.D. obtained from two independent experiments.

The mean size and surface charge of non-pegylated lipoplexes were slightly higher than the corresponding liposomes (111-140 nm and > +38 mV) (Figure 13), and despite of the increased polydispersity of the population, the values of PdI were lower than 0.2. The post-pegylation did not increased the hydrodynamic diameter of lipoplexes and maintain the polydispersity of the dispersions, except for DODAC:MO:DC-Chol (5:4:1), where both mean size and polydispersity were increased from to 112 nm with PdI of 0.12 to 154 nm with PdI of 0.3.

Pegylation efficiently reduces the lipoplexes surface charge to around +20 mV, and no significant differences between DODAB and DODAC-based lipoplexes were observed. However, pegylation of nanoformulations including lower contents of DC-Chol (10 % in 5:4:1 formulation), seems to be more efficient in decreasing the surface charge (from 48 to 17 mV in DODAB-based and from 45 to 18 mV in DODAC-based nanoformulations)

than those with higher contents of DC-Chol (16 % in 4:1:1 formulation) (from 47 to 21 mV in DODAB-based and from 38 to 22 mV in DODAC-based nanoformulations).

c. Effect of colon fluids mimicking solution on size stability of the pegylated DODAB:MO:DC-Chol (5:4:1 and 4:1:1) siRNA-lipoplexes

Although local siRNA delivery to the intestine is an attractive approach, the components of intestinal fluids, namely intestinal and nuclease enzymes, the mucus lining, the gut flora, as well as the pH range, are significant challenges for successful siRNA delivery. Therefore, nanocarriers stability is necessary for siRNA protection and consequently efficient siRNA delivery to the target sites. Preliminary studies of lipoplexes stability in a solution, previously described[113], mimicking the colon, content was performed to evaluate the possibility of local nanoparticle administration.

The effect of the colon fluids mimicking solution in the stability of pegylated DODAB:MO:DC-Chol lipoplexes was evaluated by Dynamic Light Scattering and is presented in Figure 15.

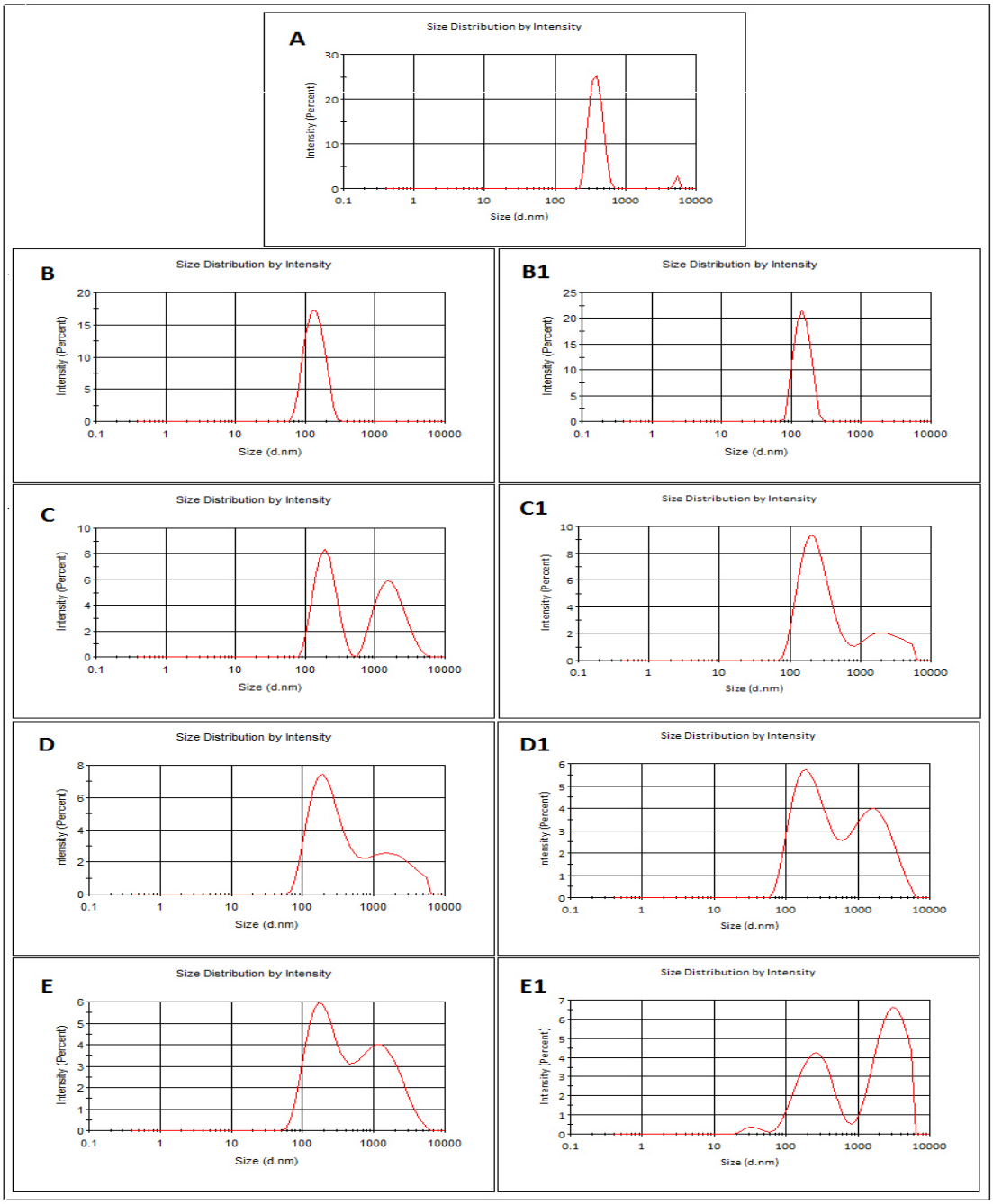

Figure 15. Effects of a colon fluid mimicking solution in the stability of pegylated DODAB:MO:DC-Chol siRNA-lipoplexes. Colon fluid (A); DODAB:MO:CH-Chol lipoplexes (5:4:1) (B) and DODAB:MO:CH-Chol (4:1:1) lipoplexes (B1) in HEPES buffer measurements after 24 h at 37 ˚C; DODAB:MO:CH-Chol lipoplexes (5:4:1) (C) and DODAB:MO:CH-Chol (4:1:1) lipoplexes (C1) incubated in colon fluid mimicking solution at time point zero; DODAB:MO:CH-Chol lipoplexes (5:4:1) (D) and DODAB:MO:CH-Chol (4:1:1) lipoplexes (D1) incubated in colon fluid mimicking solution during 30 min at 37 °C; DODAB:MO:CH-Chol lipoplexes (5:4:1) (E) and DODAB:MO:CH-Chol (4:1:1) lipoplexes (E1) incubated in colon fluid mimicking solution during 24 h at 37 °C. Data are presented as intensity (%) resulted from 5 measurements.

The colon fluid mimicking solution was diluted in HEPES buffer (1:1 v:v) to account for the dilution that occurs when it is incubated with the liposomes. The colon fluid

mimicking solution was found to present two major populations, where the mean size of the particles in population 1 was 365 ± 17 nm (90 % of intensity), and 5088 ± 264 nm (10 % of intensity) in population 2, with a high PdI value (0.5) (Figure 15.A).

The pegylated DODAB:MO:DC-Chol (5:4:1) and DODAB:MO:DC-Chol (4:1:1) lipoplexes exhibited mean sizes of 107 ± 3 nm and 130 ± 5 nm, respectively, with polydispersity index lower than 0.1. In order to evaluate the effect of the physiological temperature in the size stability of both lipoplexes, they were incubated in HEPES buffer (25 mM, pH 7.4) (1:1 v:v) during 24 h at 37 °C. Both pegylated DODAB:MO:DC-Chol (5:4:1) (Figure B) and DODAB:MO:DC-Chol (4:1:1) (Figure 15.B1) lipoplexes presented a similar unique population with mean sizes of 118 ± 4 nm and 132 ± 4 nm, respectively, with lower polydispersity (<0.09), similar to corresponding lipoplexes. The temperature of the body did not promote significant aggregation of the nanoparticles.

Immediately after incubation of DODAB:MO:DC-Chol (5:4:1) siRNA-lipoplexes with the colon fluid mimicking solution (1:1 v:v) (time point zero, Figure 15.D), it was possible to observe three populations: a population with mean size around 260 nm (with 60 % of intensity), a population with mean size around 2000 nm (with 30 % of intensity) and finally, a population with mean size higher than 3000 (with 10 % of intensity). After 30 min at 37 °C (Figure 15.D), the three populations were maintained. However, after 24 h (Figure 13.E) of exposure, two major populations were detected, one with a mean size around 400 nm (with 64 % intensity) and another population with mean size around 2044 nm (with 33 % intensity).

After the incubation of DODAB:MO:DC-Chol (4:1:1) lipoplexes with the mimicking colon fluid solution (1:1 v:v) (time point zero), two major populations were observed in Figure 13.C: a population 1 with mean size around 300 nm (with 78 % of intensity) and a population 2 with higher mean sizes, around 3000 nm (with 21 % of intensity). After 30 min at 37 °C (Figure 15.D), the diameter of the population 1 increased to 960 nm and the intensity diminishing to 60 %, but the intensity of the population 2 increased (40 %), maintaining a mean size around 3000 nm. After 24 h incubation (Figure 13.E), it was possible observe that the major populations maintained their mean sizes, but also, another population appeared with 70 nm of diameter (10 % of intensity).

For short periods of time, both pegylated formulations maintain their mean sizes in colon fluid mimicking solution, however, with the increase of the period of exposure,

the populations begin to aggregate, which is visible by the increase of the second population with highest mean sizes.

3. Biological validation of siRNA-delivery systems

a) Hemocompatibility of non-pegylated liposomes

The determination of the hemocompatibility of a drug delivery system is an essential pre-requisite for its systemic blood administration. The small size and unique physicochemical properties of nanocarriers may cause unknown interactions with blood, more precisely with erythrocytes. Therefore*, in vitro* evaluation of their hemocompatibility is necessary for early preclinical development. The most common test to evaluate erythrocytes interactions with nanovectors is the evaluation of hemoglobin released after incubation with blood. Hemolysis assays are generally considered valuable in testing the hemocompatibility of a drug formulation. A standard hemolysis assay was performed to evaluate the hemocompatibility of MO-based nanocarriers (Figure 16). It is worth mentioning that hemolysis percentage between 5 and 25 % are described as 'no concern'[114].

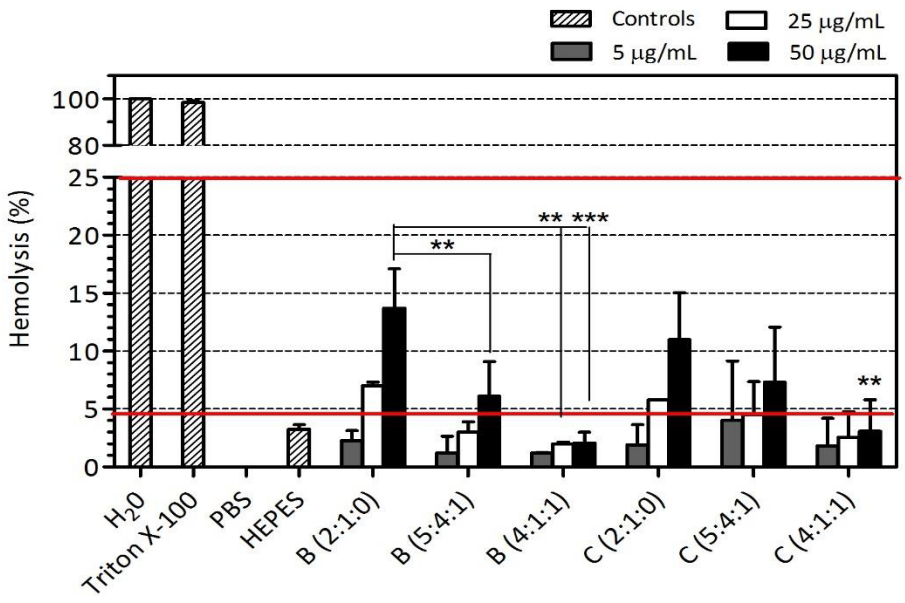

*Figure 16. Lysis of erythrocytes after 30 min of exposure to non-pegylated DODAB/C:MO:DC-Chol at 5, 25 and 50 μg/mL. DODAB:MO:DC-Chol (B) and DODAC:MO:DC-Chol (C). Data are presented as mean ± S.D. obtained from two independent experiments with freshly pig blood. The ANOVA statistical test was performed, followed by a Tukey's multiple comparison test.*p< 0.05,**p< 0.01, and***p< 0.001.*

Figure 16 shows that all MO-based nanocarriers induced low percentages of hemolysis (0-20 %). Since it is known that incubation of erythrocytes with Triton X-100 and distillated water results in around 100 % cell lysis and consequent hemoglobin release, these were used as positive controls in the hemolysis assay[114]. Figure 15 shows that HEPES buffer (pH 7.4, 25 mM) induced about 3 % of hemolysis. All MO-based nanoformulations induced significant hemolysis when compared to a negative control made with PBS buffer ($p<0,001$), with the exception of DODAB:MO:DC-Chol (5:4:1 and 4:1:1) ($p<0.05$) and DODAC:MO:DC-Chol (2:1:0 and 4:1:1) formulations ($p<0.01$) at the lowest tested concentration.

The inclusion of DC-Chol in DODAB-based nanocarriers significantly reduced the erythrocytes damage at the highest concentrations tested. Moreover, DODAB:MO:DC-Chol (16 % of DC-Chol in 4:1:1 formulation) diminished hemolysis compared with all other MO-based liposomes. The inclusion of DC-Chol in DODAC-based liposomes only reduced the damage to erythrocytes at the highest content and concentration of liposomes (16 % of DC-Chol and 50 μg/mL) ($p<0.01$). In general, DODAC-based liposomes induced a higher damage to the erythrocytes than DODAB-based liposomes, although not being statistically significant.

b. Evaluation of DODAX:MO:DC-Chol liposomes cytotoxicity

Cytotoxicity induced by pegylated and non-pegylated DODAX:MO:DC-Chol liposomes was evaluated in the colon carcinoma cell line RKO by SRB and MTT assays.

i. Effects of DODAX:MO:DC-Chol in cell proliferation

The changes in cell proliferation induced by pegylated and non-pegylated DODAX:MO:DC-Chol liposomes, at different concentrations, was evaluated by the SRB assay (Figure 17). The buffer where the nanocarriers are prepared (HEPES buffer) does not interfere with DODAX:MO:DC-Chol toxicity, neither for the higher concentrations used.

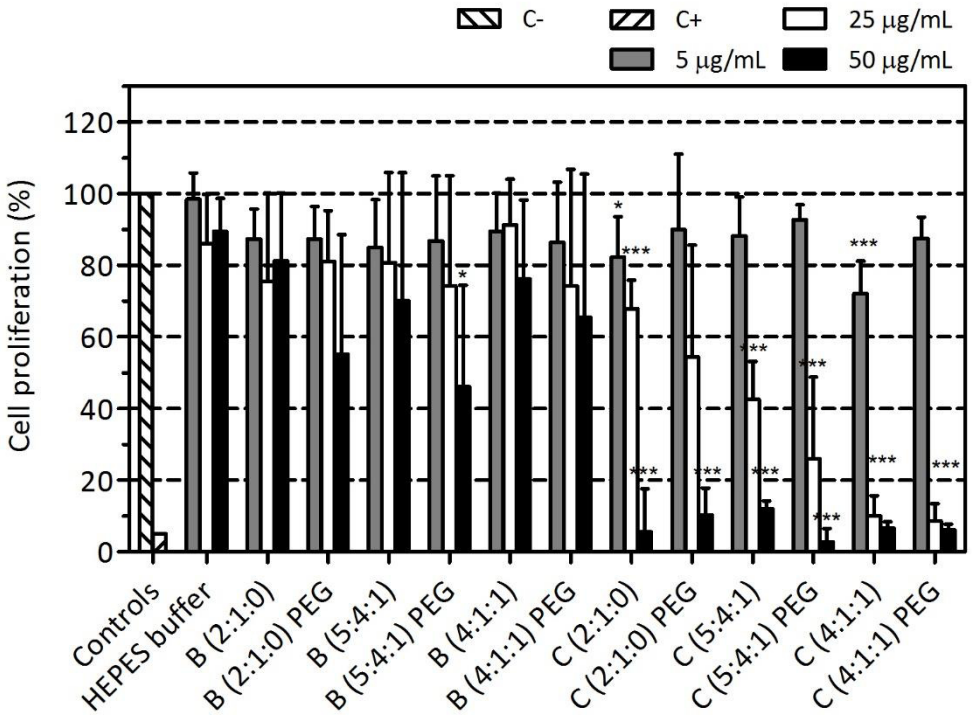

*Figure 17. Evaluation of cytotoxicity induced on cell proliferation by non pegylated and pegylated DODAB/C:MO:DC-Chol on RKO cells, as determined by SRB assay after 48 h of lipid exposure at 5, 25 and 50 μg/mL. DODAB:MO:DC-Chol (B) and DODAC:MO:DC-Chol (C). Data are presented as mean ± S.D. obtained from three independent experiments. The ANOVA statistical test was performed, followed by a Dunnett's multiple comparison test.*p< 0.05,**p< 0.01, and***p< 0.001.*

The cytotoxicity of MO-based liposomes depends on the counterion. DODAB-based liposomal formulations do not significantly reduced cell proliferation, even at higher concentrations, and the presence of DC-Chol inclusion did not significantly interfere with the DODAB-liposomes cytotoxicity.

Contrarily, a significant reduction on cell proliferation was observed for DODAC-based nanoformulations, depending on the lipids proportion and concentration. At higher concentrations (25 and 50 μg/mL), all DODAC formulations induced a significant reduction in cell proliferation ($p < 0.001$). Additionally, the increase of DC-Chol seems to increase the nanocarriers toxicity when it comes to cell proliferation. An exception was observed for the lowest concentration tested (5 μg/mL), where the presence of 10 % of DC-Chol (in formulation (5:4:1)) induced less cytotoxicity ($p<0.001$).

In general, the cell proliferation was not affected by the pegylation of the MO-based nanocarriers. Particularly, pegylated DODAB-based did not reduced cell proliferation, except for the highest concentration of DODAB:MO:DC-Chol (5:4:1) formulation when compared to control and non-pegylated formulations ($p<0.05$). In DODAC-based liposomes, only the pegylated DODAC:MO:DC-Chol (2:1:0 formulation at 5 and 25 μg/mL) and DODAC:MO:DC-Chol (4:1:1 formulation at 5 μg/mL) did not reduced cell proliferation when compared to the control cells. Also, when compared with the correspondent non-pegylated formulations (which reduced significantly cell proliferation), pegylation actually promoted some cellular proliferation.

ii. Effects of DODAX:MO:DC-Chol in cellular metabolic activity

Metabolic cytotoxicity of non-pegylated and pegylated DODAX:MO:DC-Chol delivery systems at different concentrations was evaluated by the MTT assay (Figure 18). The buffer where the nanocarriers are prepared (HEPES buffer) does not contribute to the DODAX:MO:DC-Chol liposomes toxicity, neither at higher concentrations.

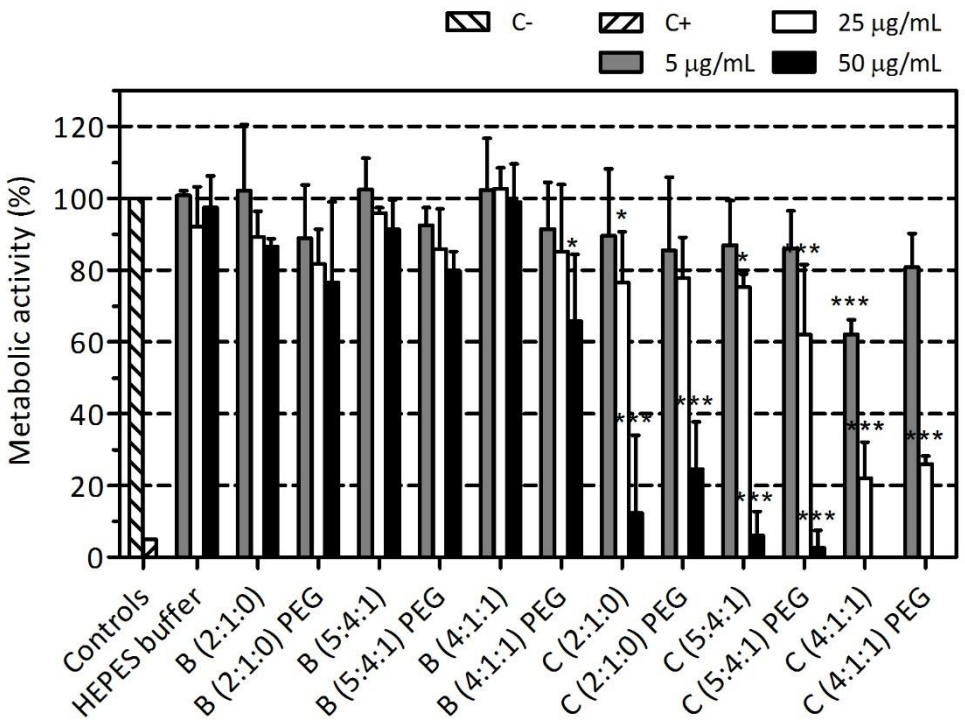

*Figure 18. Metabolic cytotoxicity induced by non pegylated and pegylated DODAB/C:MO:DC-Chol on RKO cells, evaluated by the MTT assay after 48 h of lipid exposure at 5, 25 and 50 μg/mL. DODAB:MO:DC-Chol (B) and DODAC:MO:DC-Chol (C). Data are presented as mean ± S.D. obtained from tree independent experiments. The ANOVA statistical test was performed, followed by a Dunnett's multiple comparison test.*p< 0.05,**p< 0.01, and***p< 0.001.*

Figure 18 showed that MO-based liposomes cytotoxicity was counterion-dependent. In absence of PEG, DODAB-based nanocarriers did not significantly reduce the metabolic activity of the colorectal cells (metabolic activity>75 %). The inclusion of DC-Chol had no effect on the vector toxicity compared with non-treated cells. In the case of DODAC-based nanocarriers, cytotoxicity is clearly concentration and DC-Chol dependent ($p<0.001$). In fact, even with 5 μg/mL, the formulation with the higher content of DC-Chol (16 %) already induced metabolic cytotoxicity ($p<0.001$). Moreover, increasing the concentration of the nanocarrier along with DC-Chol content, resulted in a substantial increase on the nanocarriers toxicity. DODAC:MO:DC-Chol (2:1:0) reduced the metabolic activity of the cells ($p<0.01$) at both 25 and 50 μg/mL concentrations when compared to the control cells. The inclusion of the DC-Chol at 10 or 16 % (in proportions 5:4:1 and 4:1:1, respectively) increased the significance of metabolic activity reduction ($p<0.001$).

The pegylation of DODAB:MO:DC-Chol liposomes did not induce significant levels of metabolic cytotoxicity when compared to the control cells, except in case of the

pegylated DODAB:MO:DC-Chol (4:1:1) liposomes at the highest concentration tested ($p<0.05$) compared to the non-pegylated formulation that exhibited cytotoxicity no comparing with control cells. In the case of DODAC-based formulation, non-pegylated 2:1:0 formulation, at 25 μg/mL, induced significant toxicity ($p<0.05$) while pegylated one did not interfere in metabolic toxicity when both were compared to control cell, also in non-pegylated 4:1:1 formulation, at 5 μg/mL, reduced metabolic activity significantly ($p<0.001$) while pegylated one did not interfere in metabolic activity when both were compared to control cell.

c. Cellular uptake of DODAX:MO:DC-Chol liposomes

In figure 19 is represented the percentage of fluorescent labeled liposomes internalized by RKO cells after 6 h incubation, at 37 °C.

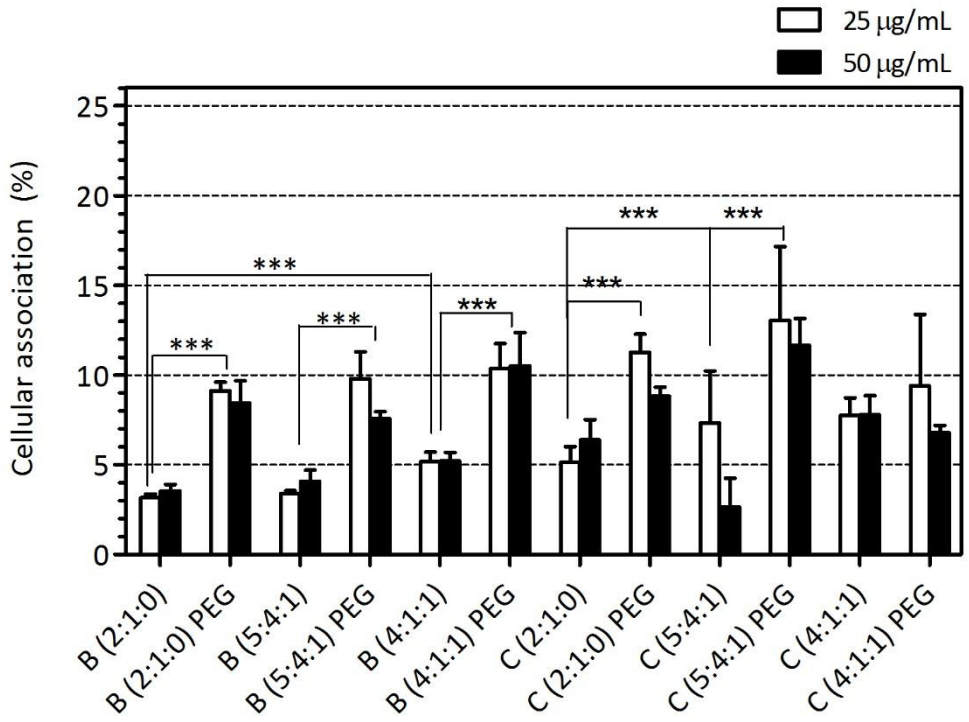

Figure 19. Evaluation of cellular uptake of non pegylated and pegylated DODAB/C:MO:DC-Chol liposomes in RKO cells, as determined by fluorescence measurements after 6 h of lipid exposure, at 25 and 50 μg/mL. DODAB:MO:DC-Chol (B) and DODAC:MO:DC-Chol (C). Data are presented as mean ± S.D. obtained from 6 experiments. The two-way ANOVA statistical test was performed, followed by a Bonferroni post-test.*$p< 0.05$,**$p< 0.01$, and***$p< 0.001$.

The cellular uptake of MO-based nanocarriers was low. Actually, less of the 20 % of the lipid added for the both concentration tested were internalized by cells. Only for

DODAC-based liposomes, the cellular uptake was concentration dependent ($p<0.001$), yet the duplication of the lipid concentration maintained or decreased the cellular uptake. Moreover, DODAC-based liposomes seems to be better internalized than DODAB-base liposomes by cells ($p<0.05$ and $p<0.001$ at 25 and 50 μg/mL, respectively).

The inclusion of DC-Chol in MO-based liposomes dispersions had a different behavior depending on the counterion. For non-pegylated DODAB-based nanocarriers a significant increase in cellular association was observed only for DODAB:MO:DC-Chol (16 % of DC-Chol in 4:1:1 nanoformulation), for both concentrations 25 and 50 μg/mL ($p<0.001$ and $p<0.01$, respectively), when compared to DODAB-based liposomes without DC-Chol. For DODAC-based liposomes, the cellular uptake only significantly increased in DODAC:MO:DC-Chol (10 % of DC-Chol in 5:4:1 nanoformulation) prepared at 25 μg/mL, when compared to DODAC:MO:DC-Chol (2:1:0). Moreover, DODAC:MO:DC-Chol 5:4:1 formulation compared with DODAB:MO:DC-Chol 5:4:1 formulation exhibited a higher cellular uptake ($p>0.001$) at 25 μg/mL, and also DODAC:MO:DC-Chol 4:1:1 nanocarrier were better internalized ($p<0.01$) when compared to DODAC:MO:DC-Chol 4:1:1 nanocarrier, at both concentrations tested.

Interestingly, cellular uptake was increased when DODAX:MO:DC-Chol liposomes were post-pegylated. In DODAB-based formulations, at both concentrations, pegylation significantly increased the nanocarriers cellular uptake ($p<0.001$). Nevertheless, in DODAC-based liposomes, some differences were observed: pegylation of liposomes significantly increased the cellular uptake of the 2:1:0 formulation ($p<0.001$), at 25 μg/mL, and of the 5:4:1 nanoformulation ($p<0.001$), at both concentrations.

d. BRAF silencing by pegylated DODAB:MO:DC-Chol siRNA-lipoplexes

DODAB:MO:DC-Chol (5:4:1; 4:1:1) nanocarriers have been demonstrated to be the more promissory vehicles for siRNA delivery revealing a suitable size for administration, a diminished cytotoxicity and aggregation and also a moderate cellular uptake. RKO cells were transfected with DODAB:MO:DC-Chol (5:4:1; 4:1:1) lipoplexes and the BRAF gene silencing efficiency was evaluated by qPCR (Figure 19).

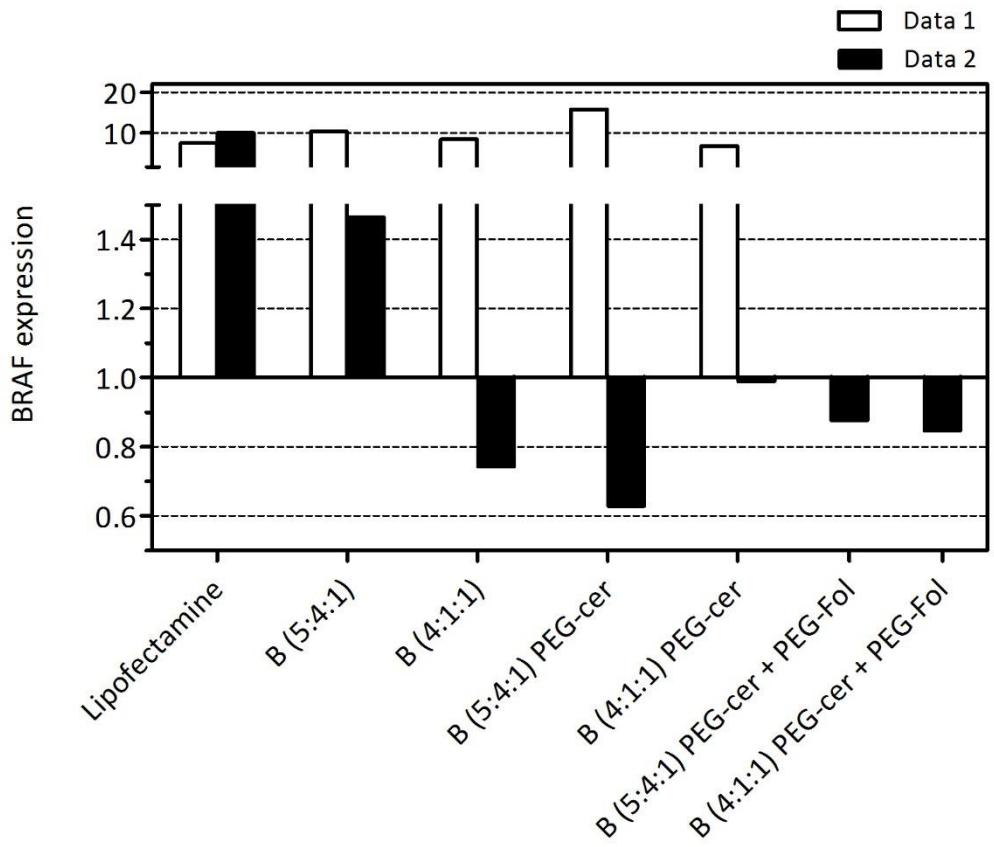

Figure 20. BRAF gene expression in RKO cells after 48 h of siRNA transfection at 100 nM. Lipofectamine 200 were used as lipofection control.The nanovectors used to transfect BRAF gene were non-pegylated and pegylated DODAB:MO:DC-Chol (5:4:1 and 4:1:1) (experience 1 corresponding to white columns); non-pegylated and pegylated DODAB:MO:DC-Chol (5:4:1 and 4:1:1) and pegylated DODAB:MO:DC-Chol (5:4:1 and 4:1:1) including 1 % PEG-FOL (experience 2 corresponding to black columns).

The transfection efficiency of MO-based nanocarriers and Lipofectamine 2000, used as a lipofection control, were compared in relation to the untreated cells, which expressed the highest level of the BRAF gene (expression value of 1). In Figure 20, it was possible to observe that in both experiences lipofectamine 2000 was not efficient in silencing the BRAF gene (expression value around 10). An unexpected increase in the expression of the BRAF gene was observed, not only for lipofectamine but also for all the conditions tested in the first experience (data 1) (expression value>1). In opposition, it was observed a reduction of the BRAF level expression by DODAB:MO:DC-Chol (4:1:1) lipoplexes (expression value<1), either non-pegylated (expression value of 0.7), pegylated with PEG-cer (expression value of 0.99) and pegylated with PEG-cer plus PEG-FOL (expression value of 0.85) in the second experience (data 2). Moreover

DODAB:MO:DC-Chol (5:4:1) pegylated with or without PEG-FOL led to a reduction of BRAF expression of 0.63 and 0.88, respectively.

Although the results obtained in the controls were not according to what was expected, this preliminary result suggest that DODAB:MO:DC-Chol might be efficient in silencing BRAF expression in CRC cells.

IV. Discussion

The need for new therapeutic approaches for specific target therapy in colorectal cancer associated with the promissory results exhibited by MO-based nanocarriers led us to develop new lipoplexes based in DODAX:MO:DC-Chol for BRAF-siRNA delivery into CRC derived cells. Indeed, MO-based liposomes have been described as efficient nanocarriers for DNA delivery[87]. It has been reported that the presence of DC-Chol enhanced the efficiency of pDNA delivery by the MO-based nanocarriers in Embryonic Kidney 293T cells without inducing significant toxicity[102]. In alternative approach, MO-based liposomes have been established as efficiently nanocarriers for siRNA delivery in H1299 eGFP cells[99]. Varying the proportion of DODAX to MO and changing the counterion from Cl^- to Br^-, altered the nanocarriers properties in such a way that not only resulted in different levels of organization, but also in internalization and different transfection efficiencies which, in turn, resulted in different gene silencing capability. Despite of dioctadecyldimethylammonium bromide (DODAB) and dioctadecyldimethylammonium chloride (DODAC) molecules only differ in the counterion (Br^- and Cl^-), its effect on bilayer hydration significantly influences several properties, like the mean size and the gel to-liquid crystalline transition temperature[96-98].

The physicochemical properties of nanocarriers largely govern the success of every gene therapy strategy. The preparation method strongly influences physicochemical characteristics of DODAX:MO:DC-Chol, such as size and surface charge, which will influence the nanocarriers pharmacokinetics and determine their success in gene delivery. Extruded MO-based liposomes demonstrated to have better physicochemical features compared with liposomes prepared by ethanol injection method[102]. In the present work, MO-based nanocarriers were produced by lipid film hydration followed by extrusion. The lipid film hydration is known to produce a heterogeneous population of multilamellar vesicles, so extrusion method was required to decrease the size and homogenize the liposome dispersion to obtain suitable SUVs and LUVs nanocarriers for biological applications. The loss of lipid during extrusion was the major drawback of this method, despite could it be quantified, it was not possible to take into account due to equipment limitations (limited access to HPLC and GS-MS and the long period of

optimization required for the techniques). MO-based nanocarriers were prepared in HEPES buffer and their physicochemical properties (size and surface charge) characterized by DLS assays. The size of the non-pegylated and pegylated DODAX:MO:DC-Chol liposomes was found to be around 100-120 nm, meeting the size requirements for the prevention of clogging of capillaries and nanocarrier extravasation throughout the fenestrae of capillaries[115]. Also, DODAB-based liposomes present a slightly higher mean size than DODAC-based liposomes, which is in accordance with the literature[99]. The counterion Br^- is less hydrated and possesses a small headgroup area than counterion Cl^-, originating weak electrostatics repulsions between DODAB headgroups leading to a decrease in the aggregate mean curvature, which is reflected by an increase in the liposomes size[116,117]. In DODAB bilayers the more tightly packed head groups hinder a homogeneous MO incorporation into the bilayers. DODAC:MO appears to form lamellar phases with less tight polar head groups, with MO better distributed, compared to DODAB:MO. Therefore, MO-rich and DODAB-rich domains are formed in DODAB:MO liposomes, as already published[99]. DSC measurements performed with this formulations reveal that DODAC:MO (2:1) presents a T_m =48 °C (ΔH=29.2 kJ/mol) and DODAB:MO (2:1) presented T_m=47.1 °C (ΔH=25.4 kJ/mol) being both characterized by the presence of lamellar phases[99]. Nevertheless, DODAC:MO (2:1) presents a higher enthalpy than DODAB:MO, which means the presence of more rigid bilayers. But not only the counterion was found to have an important effect on the structure of the liposomes, but also the MO content. As previously reported[94], in DODAX-enriched formulations (DODAX:MO (2:1)) prevails lamellar phase, while, in MO-enriched formulations (DODAX:MO (1:2)) occurs a coexistence of lamellar and nonlamellar phases. Nevertheless, the mean size of the liposomes remains approximately the same. We expected that the inclusion of a third lipid on DODAX:MO liposomes would change the liposomes properties and improve them as siRNA nanocarriers. The physicochemical characterization revealed that DC-Chol inclusion did not change the diameter of the nanoformulations. Although, a slight increase of the liposomes mean size for the higher DC-Chol content tested (16 % in 4:1:1 formulation) were observed (Figure 10), were not significant when compared with all MO-based liposomes, as previously demonstrated[102]. Differential Scanning Calorimetry (DSC) measurements performed with DODAX:MO:DC-Chol formulations (unpublished results),

reveal that DODAX:MO:DC-Chol formulations have different thermodynamics parameters depending on the counterion and DC-Chol and MO molar fraction. DODAB:MO:DC-Chol (4:1:1) presents a T_m = 43.6 °C and ΔH = 4.9 kJ/mol and DODAC:MO:DC-Chol (4:1:1) a T_m = 45.6 °C and ΔH=1.0x10^{-5} kJ/mol. For DODAB:MO:DC-Chol (5:4:1) no T_m was detected in comparison with DODAC:MO:DC-Chol (5:4:1) (T_m = 47 °C and ΔH = 7.4 kJ/mol). The presence of equal amount of DC-Chol and MO in the formulation had the ability to increase the fluidity of the bilayers for both formulations but a higher extension for DODAC based formulation. These results reinforces that in DODAB:MO based formulations, DODAB head groups are more tightly packed, hinder MO incorporation into the bilayers, resulting in the formation of MO-rich and DODAB-rich domains, the inclusion of the same amount of DC-Chol (16 %) and MO (16 %) promoting an increase in the fluidity of the lipid bilayer. These results also suggest that DODAC allows a better and more homogeneous incorporation of MO and the presence of DC-Chol supported by further decreasing the enthalpy of the system. When an excess of MO are present compared with DC-Chol (40 % MO, 10 % DC-Chol) (5:4:1) we would expect the presence of both rigid lamellar and inverted phases. Nevertheless, this result was not observed for the DODAB and DODAC based formulations. DODAC:MO:DC-Chol (5:4:1) presents a T_m=47 °C and ΔH=7.4 kJ/mol but no T_m was detected in DODAB:MO:DC-Chol (5:4:1). These results reinforces again a better distribution of MO in DODAC bilayer and that the inclusion of DC-Chol does not fluidize the membrane, instead it balances the fluidizing effect of MO. This conclusion is supported by the presence of more rigid bilayers in DODAC based system when compared to DODAB-based system. Cholesterol and derivatives of cholesterol are well-known helper lipids that can either have a stabilizing or a fluidizing effect on lipid bilayers depending on lipid content and on the lipid bilayer fluidity or rigidity[48].

The ζ-potential assays also revealed that all MO-based liposomes exhibited highly positive ζ-potentials: > +45 mV, and the inclusion of the positively charged DC-Chol content (10 % in 5:4:1 and 16 % 4:1:1 nanoformulation) did not change the surface charge of liposomes. When MO is in excess, MO is preferentially located inside bilayer while DODAB/C is located in outside bilayer. DC-Chol will be located always in outside bilayer independently of MO content, once did not self-assembly. Moreover, the positive charge is different for all MO based systems: 67 % in 2:1 formulation; 83 % in

4:1:1 formulation and 60 % in 5:4:1 formulation. Moreover, higher content of positive charge (83 %) did not resulted in higher liposomes surface charge. The positive charges also justify the good siRNA complexation observed for all formulations.

Nanocarriers ability to destabilize and fuse with the cell membrane can be determinant for endosomal escape and efficient gene silencing. Endosomal escape ability was evaluated by performing lipid mixing/fusion assay between liposomes and model membranes. All MO-based nanocarriers exhibited some fusogenic capacity, which was expectable due to their high positive charge that favored electrostatic interactions with negatively charged model endosomes, as confirmed in Figure 12. DODAC:MO:DC-Chol formulations were shown to be more fusogenic compared to DODAB:MO:DC-Chol, likely a result of the more homogeneous integration of MO in DODAC bilayers than in DODAB due to their fusogenic potential, in accordance with previous work[99]. The inclusion of DC-Chol in the formulations promoted an increase on lipid mixing/fusogenic ability of liposomes to interact with early and late endosomal models, since Chol and derivatives promote the formation of inverted non-lamellar phase contributing for destabilization of the membrane. Nevertheless, the DODAC-based liposomes seem to exhibit slightly higher fusogenicity. The absence or almost null enthalpy presented by these formulations suggests higher bilayer fluidization, which could promote good cell adhesion.

The increased lipid mixing/fusogenic events induced by DODAC:MO:DC-Chol liposomes when compared to DODAB:MO:DC-Chol liposomes are more pronounced in acidic conditions. In neutral conditions, Cl^- counterion is more hydrated than the counterion Br^-, resulting in a difference in the liposomes hydration surface, which contributes for a higher curvature of the system. Yet, this is not sufficient to promote a higher lipid mixing ability. In acidic conditions, since there are more H^+ in solution promoting the annulment of the charges, and also rescuing more the Cl^- ions than Br^+ ions, an increased lipid mixing ability exists and more fusogenic events occur for DODAC-based liposomes. Contrary to what was expected, a higher content on MO did not provide higher fusogenic capacity, supporting that fusogenic ability depends not only of the fluidity of membrane, but also on the lipid distribution in membrane.

A very important characteristic of any system for delivery purposes is its stability. We evaluated the stability of produced MO-based liposomes over 4 weeks. MO-based

liposomes exhibited a good stability in HEPES buffer solution as previously demonstrated in previous results where was demonstrated the time stability of MO-based formulations prepared in Milli Q water[102]. Highly charged cationic liposomes (ζ-potential>30 mV) exhibited colloidal stability resulting from the overcome of Van der Wall interactions by electrostatic repulsions that prevents particle aggregation making possible the prolonged storage. Although, highly charged nanocarriers strongly aggregate when exposed to physiological conditions difficulting particle administration, this can be avoided by coating them with the hydrophilic (neutral) polymer polyethyleneglycol (PEG)[118]. Previous studies by our group (unpublished results) demonstrated that the incorporation of 10 % mol of PEG-Cer chain 8 in DODAX:MO efficiently decreased siRNA-lipoplexes surface charge, improved stability in physiologic conditions without a highly reduced cellular uptake comparing with others mol percentages and higher chain of PEG-Cer, which is in accordance with previous studies[48].The ELS and DLS measurements confirmed the decrease of the liposomes surface charge in about 50 % due to the presence of PEG and a stabilization of the size. Nevertheless, the liposomes surface charge remained positively charged, as intended for the promotion of interaction and binding to cell membranes. Our results reveal a low cellular uptake significantly increased by post-pegylation of DODAX:MO:DC-Chol liposomes (Figure 19). Actually, there are several reports demonstrating that nanocarriers pegylation decrease cell uptake[119,120], but at the same time there are others that show an increase in the internalization[107]. Whether or not pegylated complexes adhere to cells depends on parameters such as the vesicle curvature and the membrane charge density (σ_M; the average charge per unit area of the membrane; controlled by the molar ratio of cationic to neutral lipid), which can be controlled by lipid choice and lipoplexes structure. At sufficiently high σ_M, electrostatic interactions “leak through” even at high levels of PEG coating, inducing attachment to the cells membrane, even when pegylation prevents aggregation of the nanocarriers[121]. Moreover, our post-pegylated lipoplexes are expected to lose the PEG-ceramides (and thus the PEG-coating) upon contact with cellular membranes and further endosomal escape. PEG-cer chain 8 already revealed little or any inhibition of cellular uptake in chinese hamster ovary cells[48]. Non-pegylated DODAC-based liposomes present a higher cellular uptake than DODAB-based liposomes. Oliveira *et al* (2014) demonstrated the opposite, that DODAB-

based liposomes were better internalized. The authors found that the reduced headgroup area of DODAB, which leads to the formation of less curved aggregates (confirmed by the higher size of the DODAB:MO liposomes compared to the DODAC:MO formulations)[99], facilitates the adherence of the nanovectors to the cell surface and increased internalization[122]. However, size is not the only explanation for cellular internalization. Actually, in our experiments, the differences in the mean size between DODAB and DODAC did not justify the higher cell adhesion of DODAC-based liposomes, and other factors have to be considered. Moreover, a higher cellular uptake of DODAX:MO:DC-Chol liposomes was obtained by the authors when compared to the cellular uptake in RKO cells. Nevertheless, the inclusion of DC-Chol in DODAX:MO liposomes increased the cellular uptake, it was always dependent onto the counterion. In DODAB:MO only at higher content of DC-Chol (16 % in 4:1:1 nanoformulation) increased cellular uptake, while in DODAC:MO this was observed only at lower DC-Chol contents (10 % in 5:4:1 nanoformulation), a fact that could be due to differences in the lipid organization and thermodynamics characteristics of the systems. Both formulations revealed a higher enthalpy reflecting the presence of greater amount of rigid nanoparticles when compared with DODAB:MO:DC-Chol (5:4:1) and DODAC:MO:DC-Chol (4:1:1) systems. The differences between our experiences and previous studies could be explained by the different cell lines used differences, RKO cells are considered hardly transfected cells when compared to H1299 eGFP cells. The incubation conditions were not the same, in fact in our work, RKO were incubated 6 h in HBSS buffer whose function is to maintain the pH, osmotic balance as well as provide water and essential inorganic ions, meaning that cells are not provided with glucose what could interfere with the normal growth of the cells. All these conditions could interfere with liposomes stability and with the way they interact with the cells. Also, low cell uptake could be explained also by sensitive issues of the method.

An effective and non-toxic delivery system is the key challenge in the development of delivery vehicles because of the off-target side effects. In addition to the cellular association analysis, we performed cytotoxicity studies of the developed systems. DODAB-based delivery systems were better tolerated by cells than their DODAC-based counterparts, which is in accordance with the literature[99]. Despite of similar physicochemical characteristics of liposomes surface, the counterion exchange

influenced the vector toxicity, especially for higher lipid concentrations. MO and DC-Chol content does not interfere with liposomal cytotoxicity, as described in previous work[102]. DC-Chol is a positively charged lipid with two amines and therefore it was expected to contribute to a higher toxicity profile, as positive charges are associated with higher cytotoxicity. However, the inclusion of different DC-Chol contents in the liposomal dispersions did not induce different ζ-potentials neither different cytotoxic effects on cell. Similarly, post-pegylation does not significantly interfere in the MO-based nanocarriers toxicity, except in DODAC-based liposomes, where a reduced toxicity was observed. Moreover, the higher capacity of the DODAC-based nanocarriers to fuse with membranes may explain the higher cell toxicity compared with DODAB-based liposomes, as they could promote a destabilization of the cell membrane, particularly in DODAC:MO:DC-Chol (4:1:1), where both lamellar and inverted phases are present associated with a high fluidity of the system. Our results also show that MO-based liposomes were more cytotoxic when evaluated by SRB assay than MTT assay as the two assays evaluate different aspects[123]. SRB assay measures cell proliferation/protein content, while MTT assay provides information about the metabolic activity of the cells that is related to the viability of the cells. Nanomaterials and nanoparticles have been evaluated by their effects on the cell lines which they can interact at different levels, such as ROS production, cell viability, cell stress, cell proliferation, cell morphology phenotyping and cell–particle uptake assays. Although, of different interaction levels we should not underestimate the sensitivity and reliability, correlation of the cytotoxicity the realistic physiological or environmental models containing cells, proteins and solutes[124].

Preclinical examination of nanoparticles biocompatibility usually requires studies of hemolysis, platelet aggregation, coagulation time, complement activation, leukocyte proliferation and uptake by macrophages[125]. Therefore, in the case of intravenous administration, evaluation of possible immediate toxic effect after exposure of nanoparticles to blood must be examined. To study some possible adverse effects on blood components, we performed an hemocompatibility assay by analyzing hemoglobin release after incubation of blood cells with DODAX:MO:DC-Chol liposomes. The surface properties of the nanoparticles play an important role and can directly damage erythrocytes membranes[126], the non-pegylated MO-based liposomes produced present

similar surface proprieties, especially in terms of surface charge. All-MO-based systems induced a percentage of hemolysis lower than 15 % and, according with several studies *in vitro*, a percentage lower than 25 % is rated as 'no concern'[125]. The red blood cells damage was diminished by the inclusion of DC-Chol in both DODAB and DODAC-based nanocarriers. Derivatives of cholesterol are described in literature as promoting stability *in vivo* and *in vitro,* which could contribute for the diminished erythrocytes damage promoted by the presence of DC-Chol. Moreover, DODAB-based delivery systems induced lower erythrocytes damage than DODAC-based formulations, which is in accordance with cytotoxicity assays, and can also be explained by the lower cell uptake of non-pegylated nanoformulations. The hemocompatibility of post-pegylated liposomes was not evaluated, as hemolysis of all MO-based liposomes was considered harmless. The fact that we had to use of pig blood instead of human blood can be a limitation of our studies as it will not give results that can be immediately translated to humans. The removal of the plasma components prior to the incubation of the erythrocytes with the liposomes is another limitation, since the adsorption of plasma proteins onto the nanocarriers surface can have an important influence on the interactions between the cells and the nanoparticles. The blood coagulation as the anticoagulant used could also contribute to false negatives, once erythrocytes in the clot cannot interact with nanovectors being protected from hemolysis. The blood clots would be removed from the supernatant by centrifugation not contributing for the hemolysis measurements. To overcome these drawbacks, the hemolysis studies should be supported with platelet aggregation studies[110]. However, this assay can already give us an indication for a good MO-based liposomes hemocompatibility and thus for a possible intravenous administration.

All MO-based nanoformulations achieved a high siRNA complexation efficiency (around 97 %) at low charge ratios (+/-) 5. Even though MO and DC-Chol induced a different degree of fluidity to the liposome bilayers, as detected by DSC assays, and consequently a different dynamic in siRNA encapsulation, the final siRNA complexation ability of the DODAX:MO:DC-Chol liposomes was not affected. The siRNA complexation is a dynamic process and, despite the degree of complexed siRNA being approximately 100 % for high charge ratios, there was no indication that the siRNA molecules were completely incorporated inside the lipoplexes nanocarriers. The mean size, PdI, as well

as ζ-potential values are parameters that can indicate whether the lipoplexes were completely formed or not. Hence, we performed DLS measurements for the siRNA-lipoplexes prepared at increasing charge ratios, and the results have shown that, a CR higher than (+/-) 7, all MO-nanocarriers features reached a plateau (supplementary material), indicating that lipoplexes were fully formed. In a post-pegylation, lipoplexes were obtained by first preparing the lipoplexes and, subsequently, coating them with PEG-ceramides chains, which spontaneously adsorb to the lipoplexes surface. So in a post-pegylation the encapsulation efficiency is not compromised and also did not interfere in lipid organization of the particle[104]. Moreover, post-pegylation process did not destabilize the liposomes hence encapsulated siRNA was not able to escape from the liposomes (unpublished results). Since it is known that an excessive amount of highly charged cationic liposomes is detrimental in terms of lipid toxicity to the cells, lipoplexes were prepared at charge ratio (+/-) 7 for cellular studies, to ensure maximum siRNA loading and low lipid-induced cytotoxicity as an excess of empty liposomes could compete with lipoplexes in cell uptake process. For all formulations, both non-pegylated and pegylated DODAX:MO:DC-Chol siRNA-lipoplexes prepared at charge ratio (+/-) 7 exhibited similar sizes (100-150 nm) and positive ζ-potentials: > +45 mV and > +17 mV, respectively. It is important to achieve a balance between siRNA protection and release from the lipoplexes to achieve biological functionality. siRNA-lipoplexes disassembly is essential to allow endosome escape and interaction with intracellular components such as RISC, in order to mediate RNA gene silencing. Depending on the type of administration, the nanocarriers will have to face different challenges. For instance, in a local rectal administration, the components of intestinal fluids, namely intestinal and nuclease enzymes, the mucus lining, the gut flora as well as the range of pH are significant challenges of successful siRNA delivery. In this study, a mimicking colon fluid (pH 6.0) was used to perform preliminary studies of lipoplexes stability for local rectal administration. The effects of mimicking colon fluid on siRNA-lipoplexes aggregation were evaluated by DLS measurements. Some reports refer that cholesterol or cholesterol derivatives, such as DC-Chol, promote *in vivo* and *in vitro* stability[100,101], in our formulations, the higher stability was reached with the pegylated siRNA-DODAB:MO:DC-Chol (5:4:1) lipoplexes containing the lower content of DC-Chol (10 %). Nevertheless, even if pegylated siRNA-lipoplexes seemed stable through a short period

of time, after 24 h of incubation, lipoplexes aggregated. Highly packed and dense lamellar structures with lower curvatures were found to be less destabilized when in physiologic mimicking conditions, and could also achieve higher transfection efficiencies[127]. As discussed above, DODAB-based lipoplexes in 4:1:1 proportion presented lamellar structures, while in 5:4:1 formulation no rigid lamellar structures were detected (absence of T_m). Despite the lipoplexes presenting lamellar phase were the less subjected to aggregation and/or disintegration, it was the formulation with both structures lamellar and inverted that presented less aggregation. Some approaches are described in the literature in order to maximize stability in complexes fluids such as colon fluid, such as coating the liposomes with polymers such poly(epsilon-caprolactone) (PCL)[41].

Finally, the BRAF expression silencing using non-pegylated and pegylated DODAB:MO:DC-Chol (5:4:1 and 4:1:1) lipoplexes was evaluated and compared to a commercial lipofection control, Lipofectamine® 2000, previously validated by our group[17]. The lipofection control did not silence BRAF expression in both experiences when analysed by qPCR. Contrariwise, lipofectamine increased the levels of BRAF expression. In one of the experiments, despite of the lipofection control did not work, BRAF expression was silenced by DODAB:MO:DC-Chol. In fact, pegylated DODAB:MO:DC-Chol (5:4:1) exhibited higher BRAF silencing comparing with all formulations even when formulations include PEG-ceramide and a possible target such as PEG-Folate that improves internalization when Folate is overexpressed in cells. The overexpression of BRAF with the control of lipofection, is difficult to explain although it might be due to damages in siRNA or in the lipofectamine or in the qPCR primers. In previous experiment we used GAPDH gene as an endogenous control that has been used in literature to normalize BRAF expression, however, BRAF expression levels were always above cell control (supplementary materials). In subsequent experiences mitochondrial gene, MT-ATP6 gene were used to normalize expression of the gene, wherein the experiments, BRAF levels were below cell control. We can hypothesize that BRAF siRNA could be damaged or promoted unspecific interactions or the qPCR BRAF primers were not appropriated/specific for BRAF amplification and could be detecting genomic DNA.

V. Conclusion and future perspectives

The work described here has important implications for the design of new nanocarriers for siRNA delivery. The combination of the nanocarriers components must be carefully optimized, once liposomal structural organization and membrane properties were highly dependent on the specific mixture between the neutral lipid MO and the cationic lipid DODAC or DODAB and DC-Cholesterol. Previous studies demonstrated that hanging the counterion Cl^- by Br^- altered the nanocarriers properties in such a way that defined the silencing efficiency. All MO-based liposomes exhibited similar physiochemical characteristics such as size and surface charge. All MO-based nanocarriers exhibited some fusogenic capacity, which was expectable due to their high positive charge that favored electrostatic interactions to anionic model endosomes. DODAC-based liposomes also presented higher fusogenic capacity than DODAB-based liposomes mainly, with the inclusion of DC-Chol (16 % in 4:1:1 nanoformulation). The more homogeneous distribution of MO and also DODAC hydration surface may explain the higher fusogenic capacity, more pronounced in acidic conditions. Also, all nanocarriers formulations achieved good complexation efficiency at lower charge ratios. Post-pegylation efficiently decrease liposomes and lipoplexes surface charge without alter particle features. The nanocarriers remain positively charged for further cell adhesion. Moreover, post-pegylation increased cellular uptake of all MO-based nanovectors, with DODAC-based liposomes achieving better ratios of internalization than DODAB-based liposomes. However, DODAC-based nanocarriers are massively toxic in RKO cells, mainly in higher tested concentrations which could be also explained by higher fusogenic capacity. Our preliminaries studies of local and intravenous administration were performed and showed that all MO-based nanovectors exhibited lower values of hemolysis (<20 %), which is rated as 'no concern' for intravenous administration. Also, the size aggregation of the pegylated DODAB:MO:DC-Chol (5:4:1 and 4:1:1) lipoplexes, for being the more promissory nanocarriers, were evaluated in a mimicking colon fluid solution (pH 6) for a possible local administration, yet, formulations seems to aggregate in this physiological conditions after a long period of exposure.

The BRAF silencing quantification by qPCR for the developed nanocarriers needs further optimization. Although, our preliminary results suggest that DODAB:MO:DC-Chol (5:4:1 and 4:1:1) could be a promissory nanovectors for a specific siRNA therapy for CRC.

Several assays should be performed in order to obtain a “proof of concept”. Considering BRAF silencing optimization using the produced nanocarriers, BRAF protein expression should also be analyzed by Western Blot in order to confirm a technical problem in the siRNA oligos or in the qPCR. After optimization of the silencing we should analyze some phenotypic alterations already associated to BRAF inhibition such as apoptotic and proliferative assays. Moreover, mimicking intestinal fluids could be used to incubate cells in the same the conditions of intestine and further evaluate the transfection efficiency. Considering the nanoparticles techniques, such as confocal and flow cytometry, should be performed to evaluate liposomes and lipoplexes cellular uptake using specific markers of endocytic pathways: clathrin-mediated and caveolae-mediated endocytosis and macropinocytosis. Moreover, intracellular trafficking and interactions of the nanocarriers should be analyzed using a quantitative method based on spatio-temporal image correlation spectroscopy (STICS) that allows for characterizing the mode of motion of nanocarriers and for quantifying their transport parameters as they move through the cytosol in a living cell. Additionally, a more physicochemical characterization of the nanocarriers should be performed to correlate the physicochemical characteristics of the nanocarriers with the efficiency in siRNA delivery, for a better understand of all process resulting in improved nanovectors design. Assays such as small angle x-ray scattering to analyze the liposomes and lipoplexes structures, as differential scanning calorimetry of the lipoplexes to understand how siRNA interfere in the fluidity of the system, as well as its implications. Also, endonucleases and protection assays should be performed to evaluate the capacity of the nanocarriers in siRNA protection in different physiological mediums using fluorescence correlations spectroscopy and correlate to the different lipid organization as its structures.

Summing up DODAB:MO:DC-Chol lipoplexes developed in this work are promising formulations for siRNA delivery into RKO CRC cells, although, further tests will be necessary for the validation of these nanocarriers. These formulations might bring new avenues for siRNA gene silencing as a therapeutic approach in CRC.

VI. References

1 Doane, T. L. & Burda, C. The unique role of nanoparticles in nanomedicine: imaging, drug delivery and therapy. *Chemical Society Reviews* **41**, 2885-2911 (2012).

2 Sanna, V., Pala, N. & Sechi, M. Targeted therapy using nanotechnology: focus on cancer. *International Journal of Nanomedicine* **9**, 467 (2014).

3 Hanahan, D. & Weinberg, Robert A. Hallmarks of Cancer: The Next Generation. *Cell* **144**, 646-674 (2011).

4 Karakosta, A., Charalabopoulos, A., Peschos, D., Batistau, A. & Charalabopoulos, K. Genetic models of human cancer as a multistep process. Paradigm models of colorectal cancer, breast cancer and chronic myelogenous and acute lymphoblastic leukaemia. *Journal of Experimental & Clinical Cancer Research* **24**, 05-14 (2005).

5 Cunningham, J. M. *et al.* Hypermethylation of the hMLH1 promoter in colon cancer with microsatellite instability. *Cancer Research* **58**, 3455-3460 (1998).

6 Takayama, T., Miyanishi, K., Hayashi, T., Sato, Y. & Niitsu, Y. Colorectal cancer: genetics of development and metastasis. *Journal of Gastroenterology* **41**, 185-192 (2006).

7 Seruca, R. *et al.* Unmasking the role of KRAS and BRAF pathways in MSI colorectal tumors. *Expert Review of Gastroenterology & Hepatology: 2007* **3**, 5-9 (2009).

8 Lao, V. V. & Grady, W. M. Epigenetics and colorectal cancer. *Nature Reviews Gastroenterology and Hepatology* **8**, 686-700 (2011).

9 Chu, E. *New treatment strategies for metastatic colorectal cancer*. (CMP Medica, 2008).

10 Krasinskas, A. M. EGFR signaling in colorectal carcinoma. *Pathology Research International* **2011** (2011).

11 Mendelsohn, J. & Baselga, J. Status of epidermal growth factor receptor antagonists in the biology and treatment of cancer. *Journal of Clinical Oncology* **21**, 2787-2799 (2003).

12 Amado, R. G. *et al.* Wild-type KRAS is required for panitumumab efficacy in patients with metastatic colorectal cancer. *Journal of Clinical Oncology* **26**, 1626-1634 (2008).

13 Ebos, J. M. *et al.* Accelerated metastasis after short-term treatment with a potent inhibitor of tumor angiogenesis. *Cancer Cell* **15**, 232-239 (2009).

14 Allegra, C. J. *et al.* Initial safety report of NSABP C-08: a randomized phase III study of modified FOLFOX6 with or without bevacizumab for the adjuvant treatment of patients with stage II or III colon cancer. *Journal of Clinical Oncology* **27**, 3385-3390 (2009).

15 Santarpia, L., Lippman, S. M. & El-Naggar, A. K. Targeting the MAPK-RAS-RAF signaling pathway in cancer therapy. *Expert Opinion on Therapeutic Targets* **16**, 103-119 (2012).

16 Davies, H. *et al.* Mutations of the BRAF gene in human cancer. *Nature* **417**, 949-954 (2002).

17 Preto, A. *et al.* BRAF provides proliferation and survival signals in MSI colorectal carcinoma cells displaying BRAFV600E but not KRAS mutations. *The Journal of Pathology* **214**, 320-327 (2008).

18 Tan, Y. H. *et al.* Detection of BRAF V600E mutation by pyrosequencing. *Pathology* **40**, 295-298 (2008).
19 Hauschild, A. *et al.* Results of a phase III, randomized, placebo-controlled study of sorafenib in combination with carboplatin and paclitaxel as second-line treatment in patients with unresectable stage III or stage IV melanoma. *Journal of Clinical Oncology* **27**, 2823-2830 (2009).
20 Wu, J. & Zhu, A. X. Targeting insulin-like growth factor axis in hepatocellular carcinoma. *Journal of Hematology & Oncology* **4**, 30 (2011).
21 Stenner, F. *et al.* A pooled analysis of sequential therapies with sorafenib and sunitinib in metastatic renal cell carcinoma. *Oncology* **82**, 333-340 (2012).
22 Roth, A. D. *et al.* Prognostic role of KRAS and BRAF in stage II and III resected colon cancer: results of the translational study on the PETACC-3, EORTC 40993, SAKK 60-00 trial. *Journal of Clinical Oncology* **28**, 466-474 (2010).
23 Richman, S. D. *et al.* KRAS and BRAF mutations in advanced colorectal cancer are associated with poor prognosis but do not preclude benefit from oxaliplatin or irinotecan: results from the MRC FOCUS trial. *Journal of Clinical Oncology* **27**, 5931-5937 (2009).
24 Kopetz, S. *et al.* PLX4032 in metastatic colorectal cancer patients with mutant BRAF tumors. *Journal of Clinical Oncology* **28**, 3534 (2010).
25 Di Nicolantonio, F. *et al.* Wild-type BRAF is required for response to panitumumab or cetuximab in metastatic colorectal cancer. *Journal of Clinical Oncology* **26**, 5705-5712 (2008).
26 Huang, T., Karsy, M., Zhuge, J., Zhong, M. & Liu, D. B-Raf and the inhibitors: from bench to bedside. *Journal of Hematology & Oncology* **6**, 30 (2013).
27 Joseph, E. W. *et al.* The RAF inhibitor PLX4032 inhibits ERK signaling and tumor cell proliferation in a V600E BRAF-selective manner. *Proceedings of the National Academy of Sciences* **107**, 14903-14908 (2010).
28 Su, F. *et al.* Resistance to selective BRAF inhibition can be mediated by modest upstream pathway activation. *Cancer Research* **72**, 969-978 (2012).
29 Elbashir, S. M. *et al.* Duplexes of 21-nucleotide RNAs mediate RNA interference in cultured mammalian cells. *Nature* **411**, 494-498 (2001).
30 Fire, A. *et al.* Potent and specific genetic interference by double-stranded RNA in Caenorhabditis elegans. *Nature* **391**, 806-811 (1998).
31 Bernstein, E., Caudy, A. A., Hammond, S. M. & Hannon, G. J. Role for a bidentate ribonuclease in the initiation step of RNA interference. *Nature* **409**, 363-366 (2001).
32 Whitehead, K. A., Langer, R. & Anderson, D. G. Knocking down barriers: advances in siRNA delivery. *Nature Reviews Drug Discovery* **8**, 129-138 (2009).
33 Yin, H. *et al.* Non-viral vectors for gene-based therapy. *Nature Reviews Genetics* **15**, 541-555 (2014).
34 Matranga, C., Tomari, Y., Shin, C., Bartel, D. P. & Zamore, P. D. Passenger-strand cleavage facilitates assembly of siRNA into Ago2-containing RNAi enzyme complexes. *Cell* **123**, 607-620 (2005).
35 Rand, T. A., Petersen, S., Du, F. & Wang, X. Argonaute2 cleaves the anti-guide strand of siRNA during RISC activation. *Cell* **123**, 621-629 (2005).
36 Hutvágner, G. & Zamore, P. D. A microRNA in a multiple-turnover RNAi enzyme complex. *Science* **297**, 2056-2060 (2002).

37 Layzer, J. M. *et al.* In vivo activity of nuclease-resistant siRNAs. *RNA* **10**, 766-771 (2004).
38 Chernolovskaya, E. L. & Zenkova, M. A. Chemical modification of siRNA. *Current Opinion in Molecular Therapeutics* **12**, 158-167 (2010).
39 Akinc, A. *et al.* Targeted delivery of RNAi therapeutics with endogenous and exogenous ligand-based mechanisms. *Molecular Therapy* **18**, 1357-1364 (2010).
40 Koynova, R. & MacDonald, R. C. Lipid transfer between cationic vesicles and lipid–DNA lipoplexes: Effect of serum. *Biochimica et Biophysica Acta (BBA)-Biomembranes* **1714**, 63-70 (2005).
41 O'Neill, M. J., Bourre, L., Melgar, S. & O'Driscoll, C. M. Intestinal delivery of non-viral gene therapeutics: physiological barriers and preclinical models. *Drug Discovery Today* **16**, 203-218 (2011).
42 Alexis, F., Pridgen, E., Molnar, L. K. & Farokhzad, O. C. Factors affecting the clearance and biodistribution of polymeric nanoparticles. *Molecular Pharmaceutics* **5**, 505-515 (2008).
43 Bazile, D. *et al.* Stealth Me. PEG-PLA nanoparticles avoid uptake by the mononuclear phagocytes system. *Journal of Pharmaceutical Sciences* **84**, 493-498 (1995).
44 Martina, M.-S. *et al.* The *in vitro* kinetics of the interactions between PEG-ylated magnetic-fluid-loaded liposomes and macrophages. *Biomaterials* **28**, 4143-4153 (2007).
45 Deshpande, M. C. *et al.* The effect of poly (ethylene glycol) molecular architecture on cellular interaction and uptake of DNA complexes. *Journal of Controlled Release* **97**, 143-156 (2004).
46 Harvie, P., Wong, F. M. & Bally, M. B. Use of poly (ethylene glycol)–lipid conjugates to regulate the surface attributes and transfection activity of lipid–DNA particles. *Journal of Pharmaceutical Sciences* **89**, 652-663 (2000).
47 Song, L. *et al.* Characterization of the inhibitory effect of PEG-lipid conjugates on the intracellular delivery of plasmid and antisense DNA mediated by cationic lipid liposomes. *Biochimica et Biophysica Acta (BBA)-Biomembranes* **1558**, 1-13 (2002).
48 Shi, F. *et al.* Interference of poly (ethylene glycol)–lipid analogues with cationic-lipid-mediated delivery of oligonucleotides; role of lipid exchangeability and non-lamellar transitions. *Biochemical Journal* **366**, 333-341 (2002).
49 Kay, M. A. State-of-the-art gene-based therapies: the road ahead. *Nature Reviews Genetics* **12**, 316-328 (2011).
50 Baum, C., Kustikova, O., Modlich, U., Li, Z. & Fehse, B. Mutagenesis and oncogenesis by chromosomal insertion of gene transfer vectors. *Human Gene Therapy* **17**, 253-263 (2006).
51 Bessis, N., GarciaCozar, F. & Boissier, M. Immune responses to gene therapy vectors: influence on vector function and effector mechanisms. *Gene Therapy* **11**, S10-S17 (2004).
52 Waehler, R., Russell, S. J. & Curiel, D. T. Engineering targeted viral vectors for gene therapy. *Nature Reviews Genetics* **8**, 573-587 (2007).
53 Bouard, D., Alazard-Dany, N. & Cosset, F. L. Viral vectors: from virology to transgene expression. *British Journal of Pharmacology* **157**, 153-165 (2009).

54 Bogdanov, A. A. Merging molecular imaging and RNA interference: early experience in live animals. *Journal of Cellular Biochemistry* **104**, 1113-1123 (2008).
55 Lee, H. *et al.* Molecularly self-assembled nucleic acid nanoparticles for targeted in vivo siRNA delivery. *Nature Nanotechnology* **7**, 389-393 (2012).
56 Yu, B., Zhao, X., Lee, L. J. & Lee, R. J. Targeted delivery systems for oligonucleotide therapeutics. *The AAPS Journal* **11**, 195-203 (2009).
57 Torchilin, V. P. Recent advances with liposomes as pharmaceutical carriers. *Nature Reviews Drug Discovery* **4**, 145-160 (2005).
58 Zhao, X. B. & Lee, R. J. Tumor-selective targeted delivery of genes and antisense oligodeoxyribonucleotides via the folate receptor. *Advanced Drug Delivery Reviews* **56**, 1193-1204 (2004).
59 Xia, W. & Low, P. S. Folate-targeted therapies for cancer. *Journal of medicinal chemistry* **53**, 6811-6824 (2010).
60 Low, P. S., Henne, W. A. & Doorneweerd, D. D. Discovery and development of folic-acid-based receptor targeting for imaging and therapy of cancer and inflammatory diseases. *Accounts of Chemical Research* **41**, 120-129 (2007).
61 Daniels, T. R., Delgado, T., Rodriguez, J. A., Helguera, G. & Penichet, M. L. The transferrin receptor part I: Biology and targeting with cytotoxic antibodies for the treatment of cancer. *Clinical Immunology* **121**, 144-158 (2006).
62 Daniels, T. R., Delgado, T., Helguera, G. & Penichet, M. L. The transferrin receptor part II: targeted delivery of therapeutic agents into cancer cells. *Clinical Immunology* **121**, 159-176 (2006).
63 Bareford, L. M. & Swaan, P. W. Endocytic mechanisms for targeted drug delivery. *Advanced Drug Delivery Reviews* **59**, 748-758 (2007).
64 Juliano, R. L., Ming, X. & Nakagawa, O. Cellular uptake and intracellular trafficking of antisense and siRNA oligonucleotides. *Bioconjugate Chemistry* **23**, 147-157 (2011).
65 Zuhorn, I. S., Kalicharan, R. & Hoekstra, D. Lipoplex-mediated transfection of mammalian cells occurs through the cholesterol-dependent clathrin-mediated pathway of endocytosis. *Journal of Biological Chemistry* **277**, 18021-18028 (2002).
66 Rejman, J., Oberle, V., Zuhorn, I. & Hoekstra, D. Size-dependent internalization of particles via the pathways of clathrin-and caveolae-mediated endocytosis. *Biochemical Journal* **377**, 159-169 (2004).
67 Hoekstra, D., Rejman, J., Wasungu, L., Shi, F. & Zuhorn, I. Gene delivery by cationic lipids: in and out of an endosome. *Biochemical Society Transactions* **35**, 68 (2007).
68 Torchilin, V. P. Cell penetrating peptide-modified pharmaceutical nanocarriers for intracellular drug and gene delivery. *Peptide Science* **90**, 604-610 (2008).
69 Basha, G. *et al.* Influence of cationic lipid composition on gene silencing properties of lipid nanoparticle formulations of siRNA in antigen-presenting cells. *Molecular Therapy* (2011).
70 Semple, S. C. *et al.* Rational design of cationic lipids for siRNA delivery. *Nature Biotechnology* **28**, 172-176 (2010).

71 Rozema, D. B. *et al.* Dynamic PolyConjugates for targeted in vivo delivery of siRNA to hepatocytes. *Proceedings of the National Academy of Sciences* **104**, 12982-12987 (2007).
72 Dominska, M. & Dykxhoorn, D. M. Breaking down the barriers: siRNA delivery and endosome escape. *Journal of cell science* **123**, 1183-1189 (2010).
73 Varkouhi, A. K., Scholte, M., Storm, G. & Haisma, H. J. Endosomal escape pathways for delivery of biologicals. *Journal of Controlled Release* **151**, 220-228 (2011).
74 Suh, J. *et al.* Real-time gene delivery vector tracking in the endo-lysosomal pathway of live cells. *Microscopy Research and Technique* **75**, 691-697 (2012).
75 Sahay, G. *et al.* Efficiency of siRNA delivery by lipid nanoparticles is limited by endocytic recycling. *Nature Biotechnology* **31**, 653-658 (2013).
76 Bangham, A., Standish, M. M. & Watkins, J. Diffusion of univalent ions across the lamellae of swollen phospholipids. *Journal of Molecular Biology* **13**, 238-IN227 (1965).
77 Jonsson, B. *Surfactants and polymers in aqueous solution*. (John Wiley & Sons, 1998).
78 Felgner, P. L. *et al.* Lipofection: a highly efficient, lipid-mediated DNA-transfection procedure. *Proceedings of the National Academy of Sciences* **84**, 7413-7417 (1987).
79 Malone, R. W., Felgner, P. L. & Verma, I. M. Cationic liposome-mediated RNA transfection. *Proceedings of the National Academy of Sciences* **86**, 6077-6081 (1989).
80 Santel, A. *et al.* RNA interference in the mouse vascular endothelium by systemic administration of siRNA-lipoplexes for cancer therapy. *Gene Therapy* **13**, 1360-1370 (2006).
81 Aleku, M. *et al.* Atu027, a liposomal small interfering RNA formulation targeting protein kinase N3, inhibits cancer progression. *Cancer Research* **68**, 9788-9798 (2008).
82 Landen, C. N. *et al.* Therapeutic EphA2 gene targeting in vivo using neutral liposomal small interfering RNA delivery. *Cancer Research* **65**, 6910-6918 (2005).
83 Morrissey, D. V. *et al.* Potent and persistent in vivo anti-HBV activity of chemically modified siRNAs. *Nature Biotechnology* **23**, 1002-1007 (2005).
84 Jayaraman, M. *et al.* Maximizing the potency of siRNA lipid nanoparticles for hepatic gene silencing in vivo. *Angewandte Chemie International Edition* **51**, 8529-8533 (2012).
85 Bhavsar, M. D. & Amiji, M. M. Gastrointestinal distribution and *in vivo* gene transfection studies with nanoparticles-in-microsphere oral system (NiMOS). *Journal of Controlled Release* **119**, 339-348 (2007).
86 Real-Oliveira, M. Use of Monoolein as a New Auxiliary Lipid in Lipofection. *International Patent n. WO2010/020935, WIP Organization, Editor*, 1-27 (2010).
87 Silva, J. *et al.* DODAB: monoolein-based lipoplexes as non-viral vectors for transfection of mammalian cells. *Biochimica et Biophysica Acta (BBA)-Biomembranes* **1808**, 2440-2449 (2011).
88 Silva, J. P. N. *et al.* Tunable pDNA/DODAB: MO lipoplexes: The effect of incubation temperature on pDNA/DODAB: MO lipoplexes structure and

transfection efficiency. *Colloids and Surfaces B: Biointerfaces* **121**, 371-379 (2014).

89 Kunitake, T. & Okahata, Y. A totally synthetic bilayer membrane. *Journal of the American Chemical Society* **99**, 3860-3861 (1977).

90 Benatti, C. R., Feitosa, E., Fernandez, R. M. & Lamy-Freund, M. T. Structural and thermal characterization of dioctadecyldimethylammonium bromide dispersions by spin labels. *Chemistry and Physics of Lipids* **111**, 93-104 (2001).

91 Briggs, J., Chung, H. & Caffrey, M. The temperature-composition phase diagram and mesophase structure characterization of the monoolein/water system. *Journal de Physique II* **6**, 723-751 (1996).

92 Luzzati, V. Biological significance of lipid polymorphism: the cubic phases. *Current Opinion in Structural Biology* **7**, 661-668 (1997).

93 Schulz, P. C., Rodrigez, J. L., Soltero-Martinez, F. A., Puig, J. E. & Proverbio, Z. E. Phase behaviour of dioactadecylalmmonium Bromide-water system. *Journal of Thermal Analysis* **51**, 49-62 (1998).

94 Oliveira, I. *et al.* Aggregation behavior of aqueous dioctadecyldimethylammonium bromide/monoolein mixtures: A multitechnique investigation on the influence of composition and temperature. *Journal of Colloid and Interface Science* **374**, 206-217 (2012).

95 Bhattacharya, S. & Bajaj, A. Advances in gene delivery through molecular design of cationic lipids. *Chemical Communications*, 4632-4656 (2009).

96 Feitosa, E., Barreleiro, P. & Olofsson, G. Phase transition in dioctadecyldimethylammonium bromide and chloride vesicles prepared by different methods. *Chemistry and Physics of Lipids* **105**, 201-213 (2000).

97 Feitosa, E. & Alves, F. R. The role of counterion on the thermotropic phase behavior of DODAB and DODAC vesicles. *Chemistry and Physics of Lipids* **156**, 13-16 (2008).

98 Feitosa, E., Alves, F. R., Castanheira, E. M. & Oliveira, M. E. C. R. DODAB and DODAC bilayer-like aggregates in the micromolar surfactant concentration domain. *Colloid Polym Sci* **287**, 591-599 (2009).

99 Oliveira, A. C. *et al.* Dioctadecyldimethylammonium: monoolein nanocarriers for efficient in vitro gene silencing. *ACS applied materials & interfaces* (2014).

100 Crook, K., Stevenson, B., Dubouchet, M. & Porteous, D. Inclusion of cholesterol in DOTAP transfection complexes increases the delivery of DNA to cells in vitro in the presence of serum. *Gene Therapy* **5**, 137-143 (1998).

101 Dabkowska, A. *et al.* The effect of neutral helper lipids on the structure of cationic lipid monolayers. *Journal of The Royal Society Interface* **9**, 548-561 (2012).

102 Gonçalves, O. S. L. *Development of DODAC-B: MO: DC-Chol lipoplexes as a novel non-viral method for transfection* Master thesis, University of Minho, (2012).

103 Lopes, I. E. A. *Development of stable lipoplexes DODAC-MO-PEG-FOL for delivery of nucleic acids to cells expressing folate receptor* Master thesis, University of Minho, (2013).

104 Peeters, L., Sanders, N., Jones, A., Demeester, J. & De Smedt, S. Post-pegylated lipoplexes are promising vehicles for gene delivery in RPE cells. *Journal of Controlled Release* **121**, 208-217 (2007).

105 Sahoo, H. Förster resonance energy transfer–A spectroscopic nanoruler: Principle and applications. *Journal of Photochemistry and Photobiology C: Photochemistry Reviews* **12**, 20-30 (2011).
106 Struck, D. K., Hoekstra, D. & Pagano, R. E. Use of resonance energy transfer to monitor membrane fusion. *Biochemistry* **20**, 4093-4099 (1981).
107 Manual, Z. N. S. U. Malvern Instruments Ltd. *Manual Version IM* **100**, 1.23-21.26 (2003).
108 Xu, R. *Particle characterization: light scattering methods*. Vol. 13 (Springer, 2001).
109 Oliveira, C. *et al.* BRAF mutations characterize colon but not gastric cancer with mismatch repair deficiency. *Oncogene* **22**, 9192-9196 (2003).
110 Naeye, B. *et al.* Hemocompatibility of siRNA loaded dextran nanogels. *Biomaterials* **32**, 9120-9127 (2011).
111 Ciapetti, G., Cenni, E., Pratelli, L. & Pizzoferrato, A. *In vitro* evaluation of cell/biomaterial interaction by MTT assay. *Biomaterials* **14**, 359-364 (1993).
112 Vichai, V. & Kirtikara, K. Sulforhodamine B colorimetric assay for cytotoxicity screening. *Nature Protocols* **1**, 1112-1116 (2006).
113 Lan, A. *et al.* Survival and metabolic activity of selected strains of Propionibacterium freudenreichii in the gastrointestinal tract of human microbiota-associated rats. *British Journal of Nutrition* **97**, 714-724 (2007).
114 Dobrovolskaia, M. A. *et al.* Method for Analysis of Nanoparticle Hemolytic Properties in Vitro. *Nano Letters* **8**, 2180-2187, doi:10.1021/nl0805615 (2008).
115 Braet, F. & Wisse, E. Structural and functional aspects of liver sinusoidal endothelial cell fenestrae: a review. *Comparative Hepatology* **1**, 1 (2002).
116 McGrath, K. Phase behavior of dodecyltrimethylammonium bromide/water mixtures. *Langmuir* **11**, 1835-1839 (1995).
117 Liu, C. K. & Warr, G. G. Hexagonal closest-packed spheres liquid crystalline phases stabilised by strongly hydrated counterions. *Soft Matter* **10**, 83-87 (2014).
118 Sanders, N., De Smedt, S., Cheng, S. & Demeester, J. Pegylated GL67 lipoplexes retain their gene transfection activity after exposure to components of CF mucus. *Gene Therapy* **9**, 363-371 (2002).
119 Gjetting, T. *et al.* In vitro and in vivo effects of polyethylene glycol (PEG)-modified lipid in DOTAP/cholesterol-mediated gene transfection. *International Journal of Nanomedicine* **5**, 371 (2010).
120 Kibria, G., Hatakeyama, H., Ohga, N., Hida, K. & Harashima, H. Dual-ligand modification of PEGylated liposomes shows better cell selectivity and efficient gene delivery. *Journal of Controlled Release* **153**, 141-148 (2011).
121 Majzoub, R. N. *et al.* Uptake and transfection efficiency of PEGylated cationic liposome–DNA complexes with and without RGD-tagging. *Biomaterials* **35**, 4996-5005 (2014).
122 Ma, B., Zhang, S., Jiang, H., Zhao, B. & Lv, H. Lipoplex morphologies and their influences on transfection efficiency in gene delivery. *Journal of Controlled Release* **123**, 184-194 (2007).
123 Keepers, Y. P. *et al.* Comparison of the sulforhodamine B protein and tetrazolium (MTT) assays for in vitro chemosensitivity testing. *European Journal of Cancer and Clinical Oncology* **27**, 897-900 (1991).

124 Jones, C. F. & Grainger, D. W. In vitro assessments of nanomaterial toxicity. *Advanced Drug Delivery Reviews* **61**, 438-456 (2009).
125 Dobrovolskaia, M. A. & McNeil, S. E. Immunological properties of engineered nanomaterials. *Nature Nanotechnology* **2**, 469-478 (2007).
126 Naahidi, S. *et al.* Biocompatibility of engineered nanoparticles for drug delivery. *Journal of Controlled Release* **166**, 182-194 (2013).
127 Llères, D. *et al.* Dependence of the cellular internalization and transfection efficiency on the structure and physicochemical properties of cationic detergent/DNA/liposomes. *The Journal of Gene Medicine* **6**, 415-428 (2004).

VII. Suplementary Materials

Table 1. Thermodynamic parameters of neat DODAX and DODAX:MO:DC-Chol liposomes obtained by DSC measurements (heating mode).

	T_s (ºC)	ΔH_s (kJ/mol)	$\Delta T_{1/2}$ (ºC)	T_m (ºC)	ΔH_m (kJ/mol)	$\Delta T_{1/2}$ (ºC)
DODAC:MO:DC-Chol (2:1:0)	-	-	-	48.3	29.2	0.8
DODAC:MO:DC-Chol (4:1:1)	-	-	-	45.6	$1.0x10^{-5}$	1.26
DODAC:MO:DC-Chol (5:4:1)	-	-	-	47.0	7.4	1.44
DODAB:MO:DC-Chol (2:1:0)	-	-	-	47.1	25.4	0.94
DODAB:MO:DC-Chol (4:1:1)	34.6	0.12	1.3	43.6	4.9	0.93
DODAB:MO:DC-Chol (5:4:1)	-	-	-	-	-	-

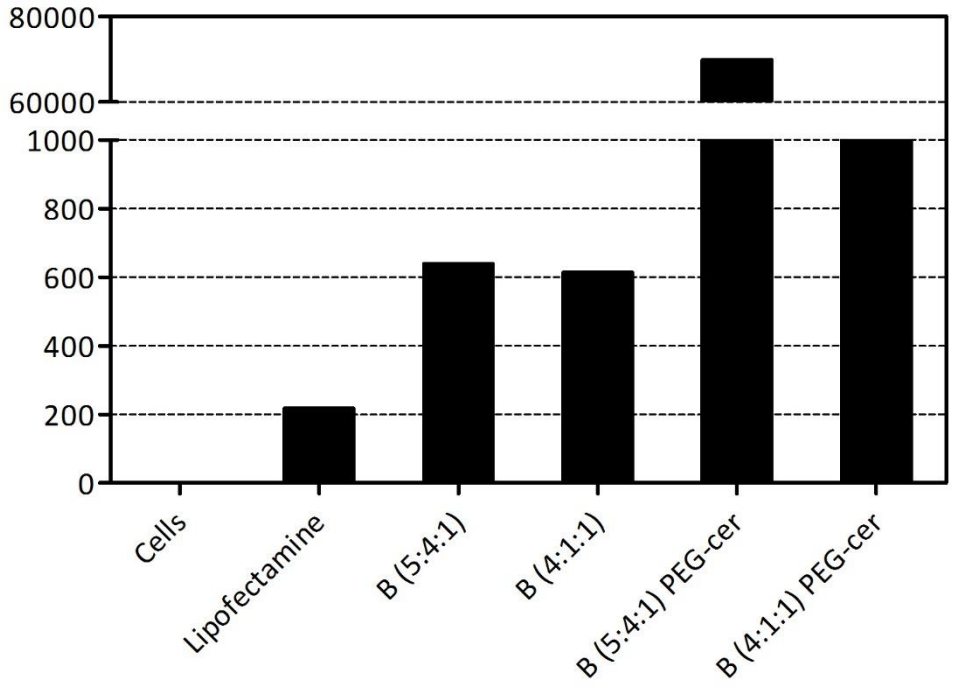

Figure 1. BRAF gene expression in RKO cells after 48 h of siRNA transfection at 100 nM. Lipofectamine 200 were used as lipofection control. The nanovectors used to transfect BRAF gene were non-pegylated and pegylated DODAB:MO:DC-Chol (5:4:1 and 4:1:1). Gene expression levels normalized with GAPDH.

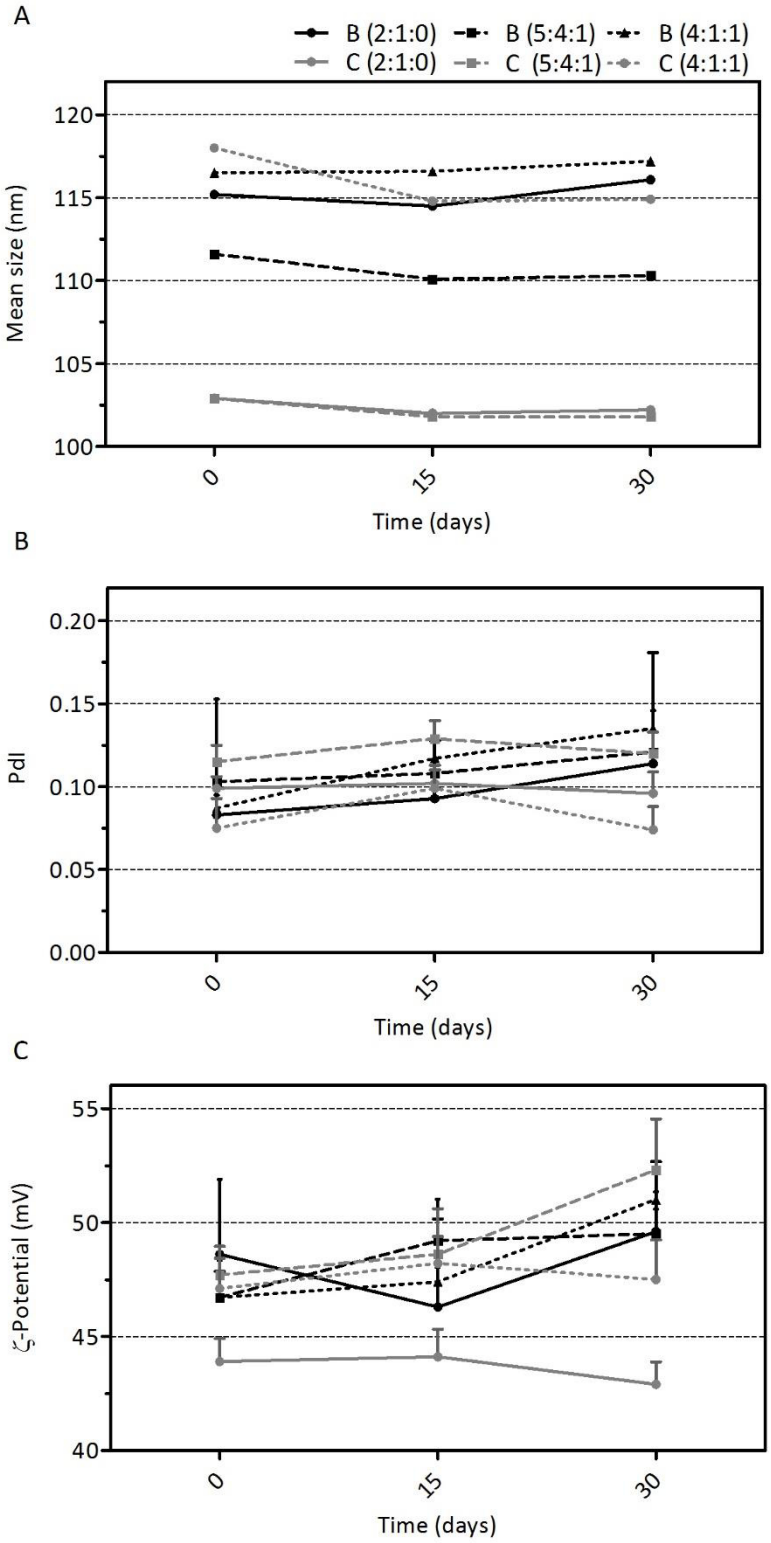

Figure 2. Physicochemical characterization of lipoplexes at different charge ratios. Z-average mean size (nm) (A); Polydispersity Index (PdI) (B) and ζ-potential (mV) (C) of DODAB/C:MO:DC-Chol liposomes over 30 days. Data are presented as mean ± S.D.